

Circulation Research

JOURNAL OF THE AMERICAN HEART ASSOCIATION

American Heart
Association® 
*Learn and Live*SM

MicroRNA-133 Controls Vascular Smooth Muscle Cell Phenotypic Switch In Vitro and Vascular Remodeling In Vivo

Daniele Torella, Claudio Iaconetti, Daniele Catalucci, Georgina M. Ellison, Angelo Leone, Cheryl D. Waring, Angela Bochicchio, Carla Vicinanza, Iolanda Aquila, Antonio Curcio, Gianluigi Condorelli and Ciro Indolfi

Circulation Research 2011, 109:880-893: originally published online August 18, 2011
doi: 10.1161/CIRCRESAHA.111.240150

Circulation Research is published by the American Heart Association, 7272 Greenville Avenue, Dallas, TX 75214

Copyright © 2011 American Heart Association. All rights reserved. Print ISSN: 0009-7330. Online ISSN: 1524-4571

The online version of this article, along with updated information and services, is located on the World Wide Web at:

<http://circres.ahajournals.org/content/109/8/880>

Data Supplement (unedited) at:

<http://circres.ahajournals.org/content/suppl/2011/08/18/CIRCRESAHA.111.240150.DC1.html>

Subscriptions: Information about subscribing to *Circulation Research* is online at
<http://circres.ahajournals.org/subscriptions/>

Permissions: Permissions & Rights Desk, Lippincott Williams & Wilkins, a division of Wolters Kluwer Health, 351 West Camden Street, Baltimore, MD 21202-2436. Phone: 410-528-4050. Fax: 410-528-8550. E-mail:
journalpermissions@lww.com

Reprints: Information about reprints can be found online at
<http://www.lww.com/reprints>

MicroRNA-133 Controls Vascular Smooth Muscle Cell Phenotypic Switch In Vitro and Vascular Remodeling In Vivo

Daniele Torella, Claudio Iaconetti, Daniele Catalucci, Georgina M. Ellison, Angelo Leone, Cheryl D. Waring, Angela Bochicchio, Carla Vicinanza, Iolanda Aquila, Antonio Curcio, Gianluigi Condorelli, Ciro Indolfi

Rationale: MicroRNA (miR)-1 and -133 play a crucial role in skeletal and cardiac muscle biology and pathophysiology. However, their expression and regulation in vascular cell physiology and disease is currently unknown.

Objective: The aim of the present study was to evaluate the role, if any, of miR-1 and miR-133 in vascular smooth muscle cell (VSMC) phenotypic switch in vitro and in vivo.

Methods and Results: We demonstrate here that miR-133 is robustly expressed in vascular smooth muscle cells (VSMCs) in vitro and in vivo, whereas miR-1 vascular levels are negligible. miR-133 has a potent inhibitory role on VSMC phenotypic switch in vitro and in vivo, whereas miR-1 does not have any relevant effect per se. miR-133 expression is regulated by extracellular signal-regulated kinase 1/2 activation and is inversely correlated with VSMC growth. Indeed, miR-133 decreases when VSMCs are primed to proliferate in vitro and following vascular injury in vivo, whereas it increases when VSMCs are coaxed back to quiescence in vitro and in vivo. miR-133 loss- and gain-of-function experiments show that miR-133 plays a mechanistic role in VSMC growth. Accordingly, adeno-miR-133 reduces but anti-miR-133 exacerbates VSMC proliferation and migration in vitro and in vivo. miR-133 specifically suppresses the transcription factor Sp-1 expression in vitro and in vivo and through Sp-1 repression regulates smooth muscle gene expression.

Conclusions: Our data show that miR-133 is a key regulator of vascular smooth muscle cell phenotypic switch in vitro and in vivo, suggesting its potential therapeutic application for vascular diseases. (*Circ Res.* 2011; 109:880-893.)

Key Words: vascular smooth muscle cells ■ microRNA ■ miR-133 ■ smooth muscle differentiation ■ vascular remodeling

Vascular smooth muscle cells (VSMCs) within adult blood vessels proliferate at a very low rate, exhibit very low synthetic activity, and express a unique repertoire of contractile proteins, ion channels, and signaling molecules.¹ Unlike skeletal muscle and cardiac muscle, which consist of terminally differentiated cells, adult VSMCs retain remarkable plasticity and can undergo rather profound and reversible changes in phenotype and growth properties in response to changes in local environmental cues. Salient examples of VSMC plasticity can be seen in response to vascular injury when VSMCs dramatically increase their proliferation, mi-

gration, and synthetic capacity, playing a critical role in vascular repair.^{1,2} A detrimental consequence of the high degree of plasticity exhibited by adult VSMCs is that it can lead to an adverse phenotypic switch and acquisition of characteristics that can contribute to development or progression of vascular disease in humans, including atherosclerosis, restenosis, cancer, and hypertension.¹⁻³

VSMC phenotypic modulation is characterized by significant changes in gene expression patterns, matrix and cytokine production, contractility, and growth state, ultimately leading to their switch from a synthetic to a proliferative phenotype.

Original received January 3, 2011; revision received August 8, 2011; accepted August 9, 2011. In July 2011, the average time from submission to first decision for all original research papers submitted to *Circulation Research* was 13.5 days.

From the Laboratory of Molecular and Cellular Cardiology, Cardiovascular Institute (D.T., C. Iaconetti, G.M.E., A.L., A.B., C.V., I.A., A.C., C. Indolfi), Magna Graecia University, Catanzaro, Italy; Research Institute for Sport and Exercise Sciences, Liverpool John Moores University (D.T., G.M.E., C.D.W.), Liverpool, United Kingdom; Istituto di Ricovero e Cura a Carattere Scientifico Multimedica (D.C., G.C.), Milan, Italy; (G.C.), Istituto di Ricerca Genetica e Biomedica, Consiglio Nazionale delle Ricerche (D.C., G.C.), Segrate, Milan, Italy.

Drs Torella and Iaconetti contributed equally to this work.

Correspondence to Daniele Torella, MD, PhD, Cardiovascular Institute, Laboratory of Molecular and Cellular Cardiology, Department of Experimental and Clinical Medicine, Magna Graecia University, Campus S. Venuta, Viale Europa, Germaneto, 88100 Catanzaro, Italy (E-mail dtorella@unicz.it); or Ciro Indolfi, MD, Cardiovascular Institute, Laboratory of Molecular and Cellular Cardiology, Department of Experimental and Clinical Medicine, Magna Graecia University, Campus S. Venuta, Viale Europa, Germaneto, 88100 Catanzaro, Italy (E-mail indolfi@unicz.it)

© 2011 American Heart Association, Inc.

Circulation Research is available at <http://circres.ahajournals.org>

DOI: 10.1161/CIRCRESAHA.111.240150

Non-standard Abbreviations and Acronyms

BrdU	bromodeoxyuridine
CTRL	controls
ERK	extracellular signal-regulated kinase
FISH	fluorescence in situ hybridization
GFP	green fluorescent protein
MAPK	mitogen-activated protein kinase
miR	microRNA
MOI	multiplicity of infection
PDGF	platelet-derived growth factor
SM	smooth muscle
SMC	smooth muscle cell
SRF	serum response factor
VSMC	vascular smooth muscle cell

Thus, understanding the regulatory mechanisms underlying the VSMC phenotypic switch is of paramount importance.¹⁻³

One of the key breakthroughs for the study of gene expression regulation has recently been the discovery of microRNAs (miRNAs or miRs) and their role in gene silencing through mRNA degradation or translational inhibition.^{4,5} Increasing evidence indicates that miRNAs regulate key genetic programs in cardiovascular biology, physiology, and disease.^{4,5} In particular, miR-21, -143, -145, -221, -222 have all been implicated to play a role in VSMC function and phenotypic plasticity.⁶⁻¹¹

More recently, 2 articles demonstrated that miR-1 is induced by myocardin overexpression in human SMCs, contributing to myocardin-dependent reduction of human SMC growth in vitro.^{12,13} miR-133a-1/miR-1-2 and miR-133a-2/miR-1-1 are 2 bicistronic miRNA clusters reported to be specifically expressed in cardiac and skeletal muscle.^{4,5} A third bicistronic miRNA cluster, comprising miR-206 and miR-133b, is expressed specifically in skeletal muscle but not in the heart.^{4,5} miR-1 (miR-1-1/miR-1-2) and miR-133 (miR-133a-1/miR-133a-2) play essential roles in cardiac and skeletal muscle development, physiology, and disease^{4,5}; however, their functions in VSMCs and vascular disease are largely unknown. Thus, the aim of the present study was to evaluate the role, if any, of miR-1 and miR-133 in VSMC phenotypic switch in vitro and in response to vascular injury in rat carotid arteries in vivo.

Methods

Adenoviruses expressing miR-1 (adeno-miR-1) and miR-133 (adeno-miR-133) were obtained as previously described.¹⁴ Anti-miR constructs were obtained from Ambion (Austin, TX). Balloon injury of the right carotid artery was performed in male Wistar rats using a Fogarty 2F arterial embolectomy catheter as described.^{15,16} miR-133 probe for FISH analysis and the PBS-formulated locked-nucleic-acid-modified anti-miR-133 were obtained from Exiqon (Woburn, MA).

An expanded Methods section is available in the online-only Data Supplement at <http://circres.ahajournals.org>.

Results

miR-1 and miR-133 Regulation in Quiescent and Proliferating VSMCs

miR-1 and miR-133 are significantly more expressed in skeletal and cardiac muscle tissue, compared with aorta, carotid artery, and bronchial SM tissue (Figure 1A to 1C). However, miR-1 was almost absent in vascular SM tissue, whereas miR-133 was expressed at levels comparable to those of some vascular enriched miRs, such as miR-221 and miR-222, but lower than those of other vascular miRs, such as miR-143 and miR-145 (Figure 1D). FISH analysis demonstrated that in carotid arteries miR-133 is specifically expressed in VSMCs (Figure 1E and Online Figure I). The latter was confirmed at the single-cell level analyzing freshly isolated adult aortic VSMCs (Figure 1E). miR-133a is mainly expressed in VSMC cytoplasm, whereas miR-133b is not expressed in VSMCs (Online Figure II).

In serum-starved synchronized quiescent adult rat aortic VSMCs ($0.5 \pm 0.5\%$ BrdU^{pos}), miR-133 was significantly more abundant than miR-1, whereas the latter had indeed almost negligible levels (Figure 1F). At the different time points after serum stimulation, miR-1 levels remained unchanged. On the other hand, miR-133 was significantly downregulated in proliferating VSMCs ($74.5 \pm 7.5\%$ and $88.5 \pm 8.5\%$ BrdU^{pos} at 24 and 48 hours, respectively), compared with their quiescent counterparts (Figure 1F). Cycling VSMCs had very low levels of miR-133 as analyzed by FISH (Figure 1G). When proliferating VSMCs were coaxed back into quiescence by serum starvation at 48 hours for a further 48 hours (total 96 hours, $3.5 \pm 2.5\%$ BrdU^{pos}), miR-133 transcripts increased back to levels comparable to those of the quiescent state of the baseline experiment at time 0 (Figure 1F).

In cardiac and skeletal muscle cells, miR-133 is regulated by several factors, including the MAPKs.¹⁷ The ras/MAPK pathway has a crucial role in promoting VSMC proliferation in vitro and in vivo.^{1,2,18} In agreement with previous findings,¹⁸ PD98059, a selective inhibitor of MAPK/ERK1/2 kinase, abolished ERK1/2 phosphorylation and VSMC proliferation on PDGF treatment (data not shown). More importantly, PD98059 treatment ($50 \mu\text{mol/L}$) significantly inhibited the PDGF-mediated downregulation of miR-133 in proliferating VSMCs (Figure 1H). On the contrary, the inhibition of MAPK/c-Jun N-terminal kinase with SP600125, MAPK/p38 with SB203580, or phosphatidylinositol 3'-OH kinase with LY294002 had no significant effect on the downregulation of miR-133 by PDGF (data not shown).

These data show that miR-133, unlike miR-1, is appreciably expressed in vascular SM tissues and cells. Importantly, miR-133 levels show physiological variation during the VSMC cycle by which miR-133 is downregulated in proliferating VSMCs in vitro. Furthermore, ERK1/2 activation is at least in part responsible for miR-133 downregulation when VSMCs are primed for the phenotypic switch in vitro.

miR-133 but Not miR-1 Modulates VSMC Proliferation In Vitro

For miR-133 or miR-1 gain-of-function experiments, VSMC were transfected with adeno-miR-133 or adeno-miR-1.¹⁴

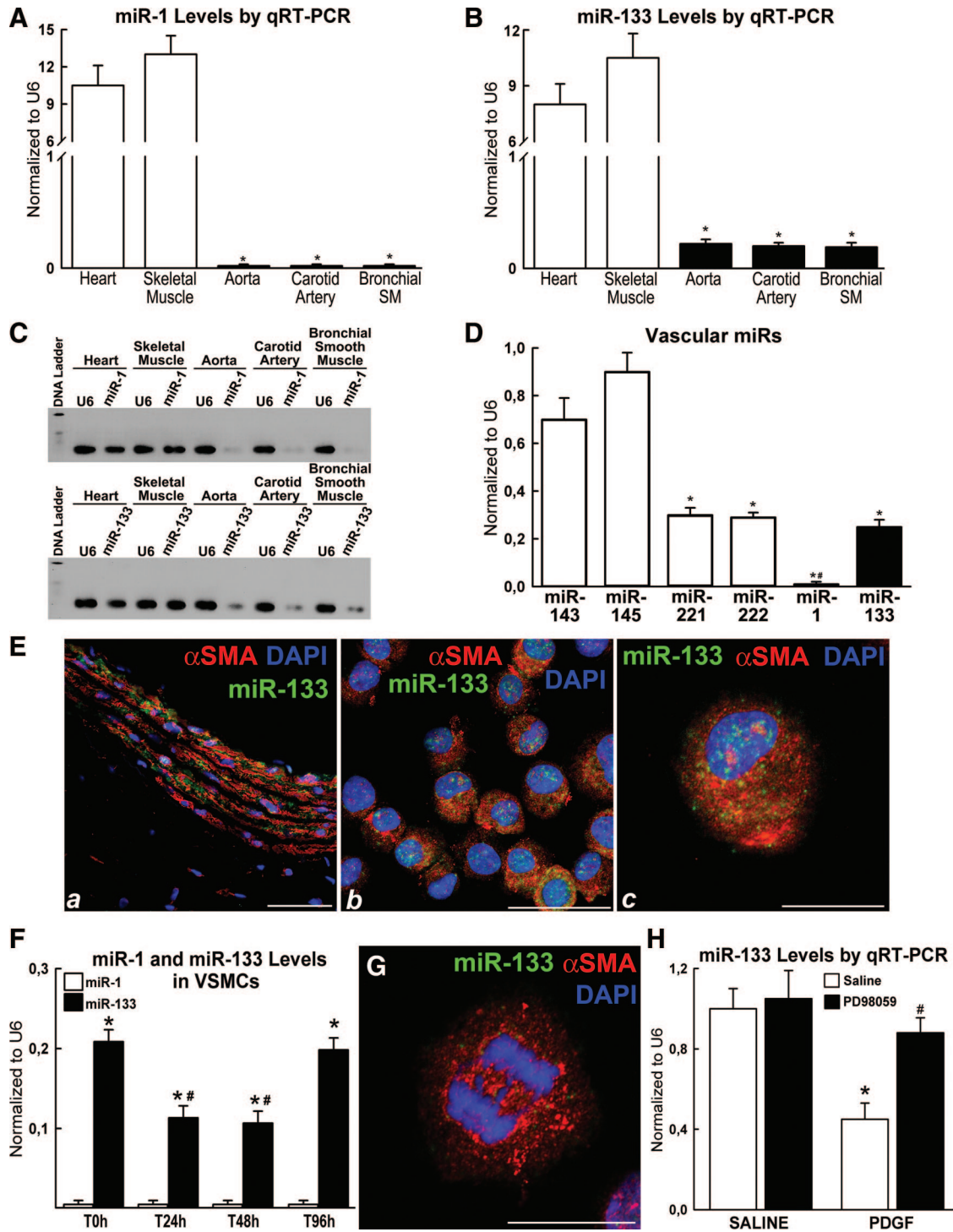


Figure 1. miR-1 and miR-133 expression and regulation in quiescent and proliferating vascular smooth muscle cells. **A** and **B**, miR-1 and miR-133 levels in adult rat vascular smooth muscle (VSM) and skeletal (Sk) muscle. **C**, Representative quantitative reverse transcription–polymerase chain reaction (qRT-PCR) gel of miR-1 and miR-133 expression. **D**, miR expression in rat carotid artery. * $P < 0.05$ vs miR-143, and -145; # $P < 0.05$ vs miR-143, -145, -221, -222, and -133. **E**, miR-133 expression in rat carotid artery (a) and isolated adult rat aortic VSMCs (b and c) (miR-133 FISH probe, green fluorescence; α -smooth muscle actin (α SMA), red; 4',6-diamidino-2-phenylindole [DAPI], nuclei stain, blue). Scale bars=50 μ m (a and b), 20 μ m (c). **F**, miR-1 and miR-133 levels at 48 hours of starvation (T0h), 24 and 48 hours (T24h and T48h) during active proliferation following 10% FBS stimulation, and 48 hours following further serum starvation (T96h). * $P < 0.05$ vs miR-1; # $P < 0.05$ vs T0 and T96 hours. **G**, miR-133 downregulation in dividing VSMCs as compared with quiescent VSMC in **E** (c). Scale bar=20 μ m. **H**, PD98059 prevents PDGF-BB-induced miR-133 downregulation. * $P < 0.05$ vs saline; # $P < 0.05$ vs PDGF.

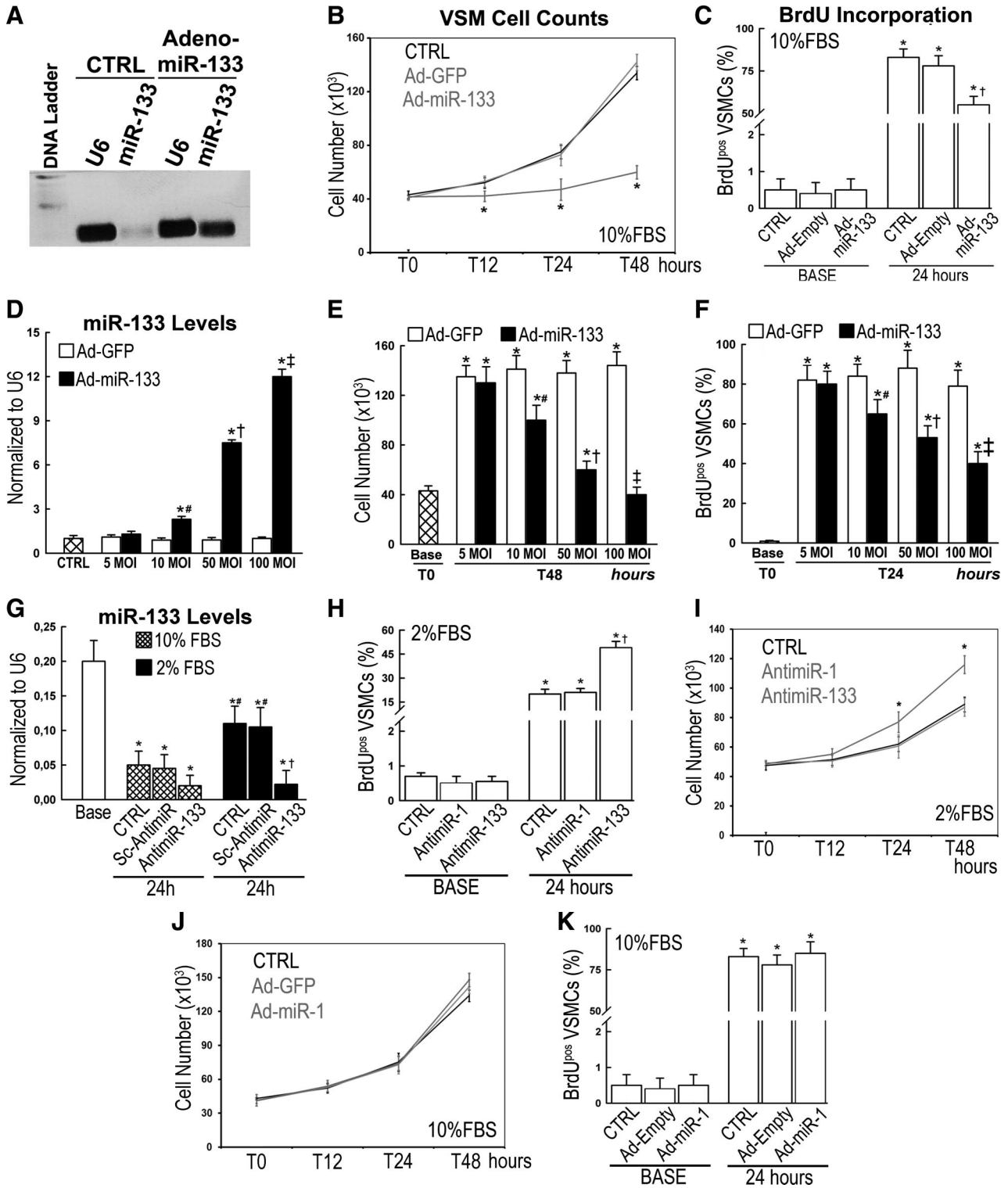


Figure 2. Effects of miR-1 or miR-133 gain and loss of function on VSMC proliferation in vitro. **A**, miR-133 overexpression by adenoviral vector transfection (Ad-miR-133). **B** and **C**, Ad-miR-133 reduced VSMC proliferation in vitro as measured by cell counts, as well as BrdU incorporation. **B**, * $P < 0.05$ vs control (CTRL) and Ad-GFP; **C**, * $P < 0.05$ vs BASE, † $P < 0.05$ vs CTRL and Ad-empty (24 hours). CTRL refers to untransfected cells. **D**, Ad-miR-133 increases miR-133 levels in a dose-dependent manner. * $P < 0.05$ vs CTRL; # $P < 0.05$ vs 5, 50, and 100 MOI; † $P < 0.05$ vs 5, 10, and 100 MOI; ‡ $P < 0.05$ vs 5, 10, and 50 MOI. **E** and **F**, Ad-miR-133 inhibits VSMC proliferation in a dose-dependent manner. * $P < 0.05$ vs base; # $P < 0.05$ vs 5, 50, and 100 MOI; † $P < 0.05$ vs 5, 10, and 100 MOI; ‡ $P < 0.05$ vs 5, 10, and 50 MOI. BASE refers to cell plates of the different groups at baseline before 10% serum stimulation (no significant difference between groups at baseline, so they were pooled and are presented together in 1 bar). **G**, Differential effects of 10% and 2% FBS media in the presence of PBS (CTRL), scrambled (Sc) anti-miR or anti-miR-133 on miR-133 expression in VSMCs in vitro. * $P < 0.05$ vs time 0 (base); # $P < 0.05$ vs CTRL and Sc-Anti-miR (10% FBS); † $P < 0.05$ vs CTRL and Sc-Anti-miR (2% FBS). **H** and **I**, Anti-miR-133 increased 2% FBS-stimulated VSMC proliferation. **H**, * $P < 0.05$ vs base; † $P < 0.05$ vs CTRL and anti-miR-1. **I**, * $P < 0.05$ vs CTRL and anti-miR-1. **J** and **K**, Ad-miR-1 did not affect VSMC proliferation in vitro. **K**, * $P < 0.05$ vs BASE.

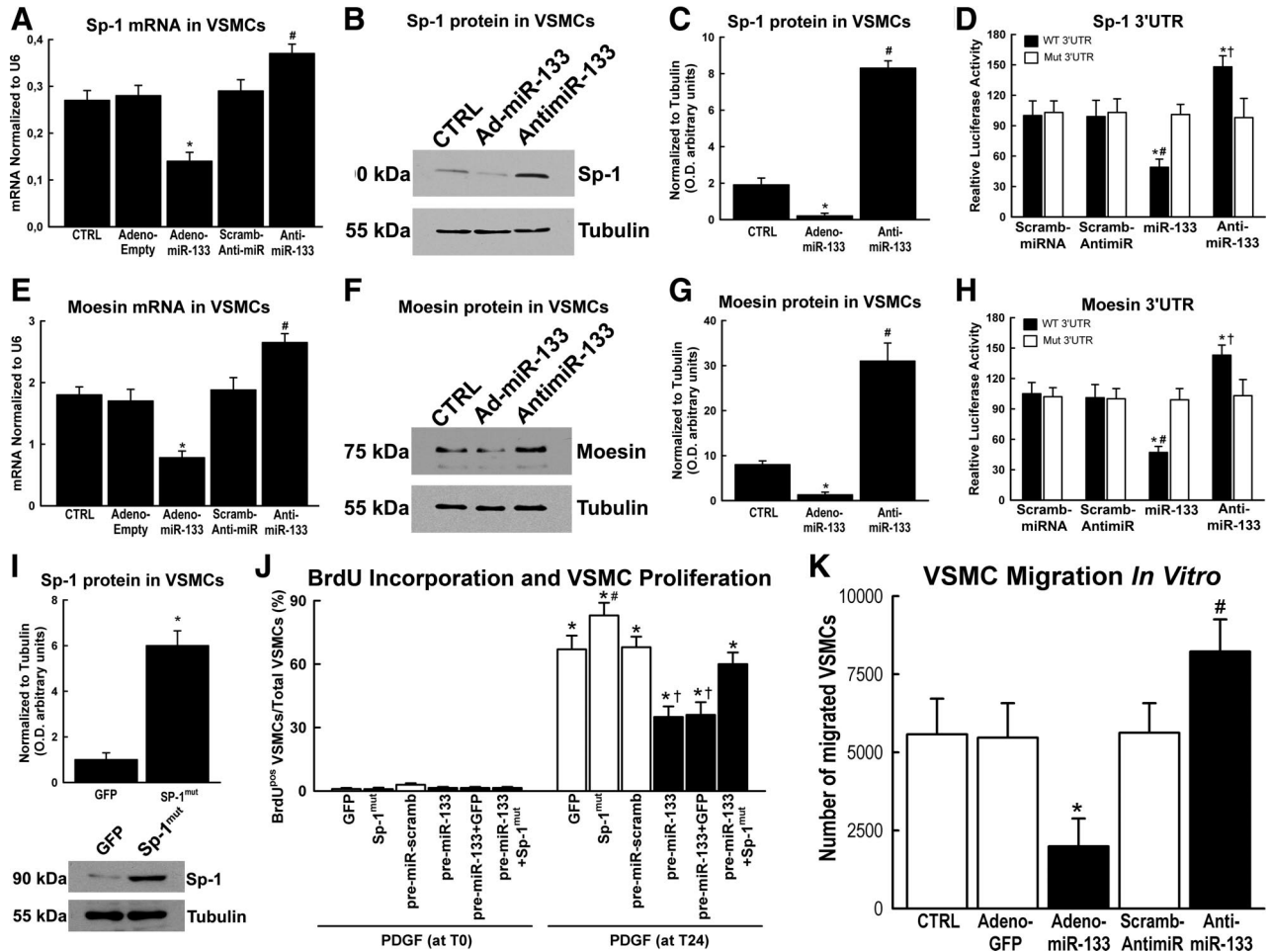
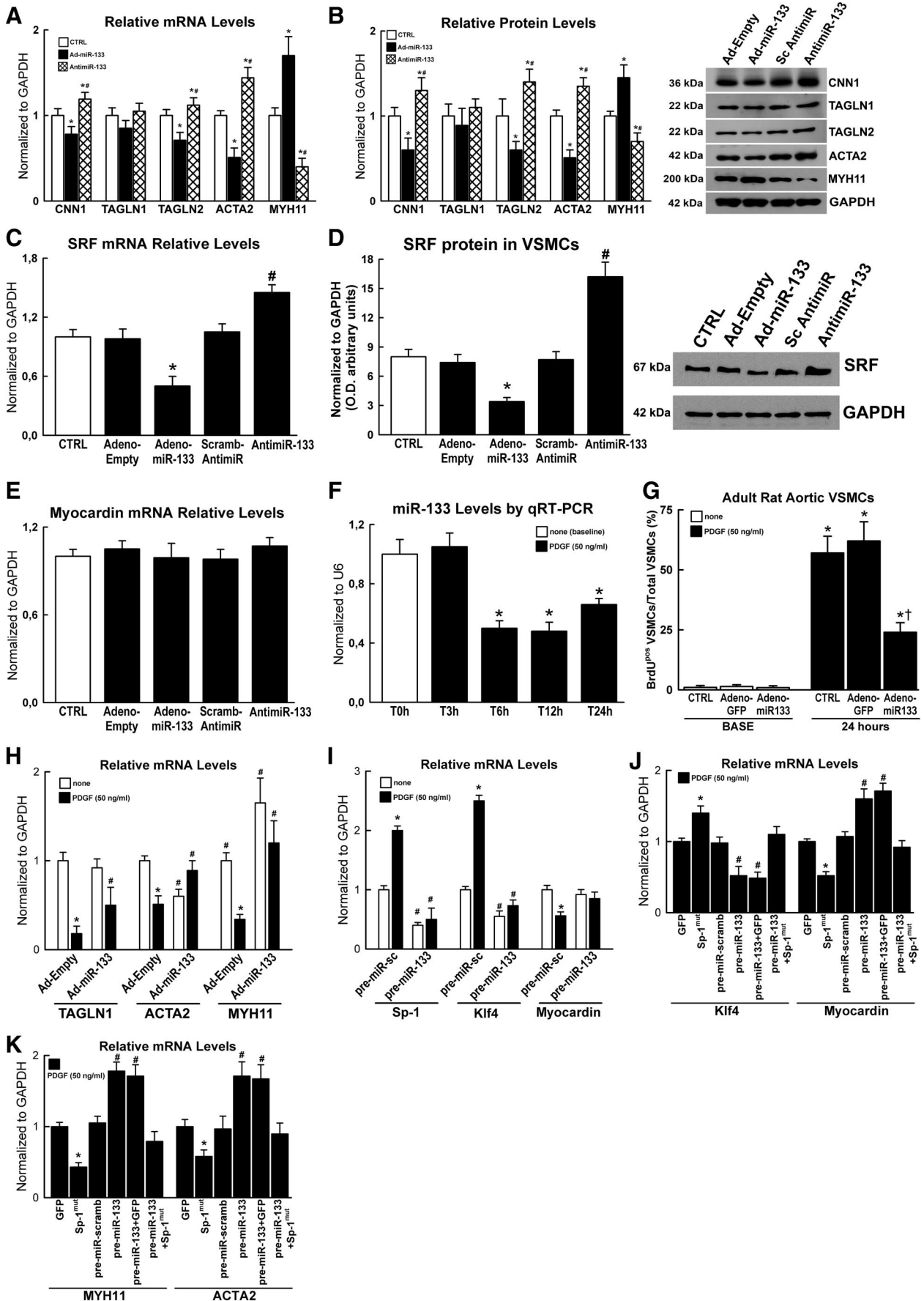


Figure 3. Targets of miR-133 in VSMC activation in vitro. **A**, Ad-miR-133 decreases and anti-miR-133 increases Sp-1 mRNA levels in VSMCs in vitro. * $P < 0.05$ vs control (CTRL), adeno-empty, scrambled (Scramb)-anti-miR, and anti-miR-133; # $P < 0.05$ vs CTRL, adeno-empty, adeno-miR-133, and Scramb-anti-miR. **B** and **C**, Ad-miR-133 decreases and anti-miR-133 increases Sp-1 protein levels in VSMCs in vitro. **C**, Optical density (OD). * $P < 0.05$ vs CTRL and anti-miR-133; # $P < 0.05$ vs CTRL and adeno-miR-133. **D**, Luciferase assay of wild-type (WT) and mutant (Mut) Sp-1 3' untranslated region (UTR) in pre-miR-133- and anti-miR-133-treated VSMCs. * $P < 0.05$ vs the respective Mut3' UTR; # $P < 0.05$ vs Scramb-miRNA, Scramb-anti-miR, and anti-miR-133; † $P < 0.05$ vs Scramb-miRNA, Scramb-anti-miR, miR-133. **E**, Ad-miR-133 decreases and anti-miR-133 increases moesin mRNA levels in VSMCs in vitro. * $P < 0.05$ vs CTRL, adeno-empty, Scramb-anti-miR, and anti-miR-133; # $P < 0.05$ vs CTRL, adeno-empty, adeno-miR-133 and Scramb-anti-miR. **F** and **G**, Ad-miR-133 decreases and anti-miR-133 increases moesin protein levels in VSMCs in vitro. **G**, * $P < 0.05$ vs CTRL and anti-miR-133; # $P < 0.05$ vs CTRL and adeno-miR-133. **H**, Luciferase activity assay for moesin 3' UTR. *, #, † $P < 0.05$ as in **D**. **I**, Sp-1 overexpression by Sp-1^{mut} construct transfection. * $P < 0.05$ vs GFP plasmid construct. **J**, Sp-1^{mut} overexpression effects on PDGF-BB-induced VSMC proliferation in the presence or absence of pre-miR-133. Pre-miR-scramb indicates scrambled pre-miR. * $P < 0.05$ vs time 0 (T0); # $P < 0.05$ vs GFP, pre-miR-scramb, pre-miR-133, pre-miR-133+GFP, and pre-miR-133+Sp-1^{mut}; † $P < 0.05$ vs GFP, Sp-1^{mut}, pre-miR-scramb, and pre-miR-133+Sp-1^{mut}. **K**, Ad-miR-133 decreases and anti-miR-133 increases VSMC migration in vitro. * $P < 0.05$ vs CTRL, adeno-GFP, Scramb-anti-miR, and anti-miR-133; # $P < 0.05$ vs CTRL, adeno-GFP, adeno-miR-133, and Scramb-anti-miR.

Control cells were transfected with adeno-GFP or adeno-empty vectors. The 2 latter adenovectors had no effect per se on VSMC molecular phenotype or growth status compared with naive untransfected control cells, and to simplify the presentation, CTRL label (primarily referring to untransfected control cells) includes these 3 group of controls if not otherwise specified. For loss-of-function experiments, we used chemically modified single stranded nucleic acids designed to specifically bind to and inhibit endogenous miR-133 (anti-miR-133) or miR-1 (anti-miR-1). A random sequence anti-miR molecule (scrambled anti-miR) served as negative control.

Forty-eight hours after successful adenoviral transfection at 50 MOI (Figure 2A and Online Figure III), VSMCs were stimulated to proliferate by 10% FBS. miR-133 overexpression significantly reduced VSMC proliferation compared with CTRL cells (Figure 2B and 2C). Importantly, adeno-miR-133 reduces VSMC proliferation at different levels of expression obtained by 10 to 100 MOIs (Figure 2D to 2F).

Anti-miR-133 administration did not affect VSMC proliferation stimulated by 10% FBS (Online Figure IV). The latter could be related to the extreme reduction of endogenous miR-133 levels in 10% FBS stimulated VSMCs (Figure 2G), which cannot be further affected by an additional exogenous



inhibition. Indeed, 2% FBS stimulation downregulates miR-133 significantly less than 10% FBS (Figure 2G). Remarkably, in the latter conditions, anti-miR-133 treatment significantly increased VSMC proliferation compared with CTRL cells (Figure 2H and 2I).

miR-1 overexpression, as well as that of anti-miR-1, did not affect VSMC proliferation in vitro (Figure 2I, 2J and 2K).

In summary, miR-133, but not miR-1, plays a significant physiological role on VSMC growth in vitro. Preventing miR-133 downregulation on proliferative switch by miR-133 overexpression reduces VSMC proliferation. On the other hand, knocking down miR-133 function increases VSMC proliferation.

Targets of miR-133 in VSMC Activation In Vitro

Searching for evolutionarily conserved targets of miR-133 by TargetScan prediction algorithms,¹⁹ we spotted the transcription factor Sp-1, which regulates VSMC phenotypic switch in vitro and is upregulated in animal models of vascular injury,^{20–22} and the actin-binding protein moesin, which regulates VSMC migration in vitro and in vivo.²³

Adeno-miR-133 caused mRNA degradation of both Sp-1 and moesin, whereas mRNA levels of the latter 2 genes were upregulated when VSMCs were treated with anti-miR-133 (Figure 3A and 3E). Accordingly, 2 specific luciferase reporters for Sp-1 and moesin were specifically repressed by exogenous miR-133 (Figure 3D and 3H). Consistent with these findings, expression of Sp-1 and moesin proteins was upregulated in VSMCs treated with anti-miR-133, whereas it was decreased in VSMCs transfected with adeno-miR-133 (Figure 3B and 3C and F-G). Thus, miR-133 directly targets for repression Sp-1 and moesin in VSMCs in vitro.

We assessed whether rescuing Sp-1 repression by miR-133 prevented miR-133 effects on VSMC proliferation. To this end, we cotransfected VSMCs with a synthetic miR-133 mimic (pre-miR-133 precursor molecule, which, similarly to adeno-miR-133, inhibits VSMC proliferation in vitro [Online Figure V]) and an Sp-1 cDNA construct mutated in the 3' untranslated region binding site for miR-133 seed region (Sp-1^{mut}), which cannot be repressed by miR-133. Sp-1^{mut} overexpression (Figure 3I) directly amplified PDGF-BB-induced VSMC proliferation in vitro (Figure 3J). More importantly, Sp-1^{mut} transduction rescued the inhibitory ef-

fects on VSMC proliferation in vitro by pre-miR-133 overexpression (Figure 3J).

Finally, as moesin, as well as Sp-1, modulates VSMC migration,^{1,22,23} we tested the hypothesis that miR-133 might also inhibit cell migration. On 2% FBS stimulation for 24 hours, adeno-miR-133 transfection resulted in a significant decrease of migrating VSMCs in the Boyden chamber. Accordingly, anti-miR-133 did increase VSMC migration (Figure 3K).

miR-133 Regulation of SM Genes In Vitro

SRF, which belongs to the MADS (MCMI, Agamous, Deficiens, SRF) transcription factor family, is known to regulate numerous cardiac, skeletal, and SM genes binding with the CARG [a CC(AT)₆GG motif] elements^{1,3} through its potent transcriptional coactivator, myocardin.²⁴ Importantly, SRF is a known target for transcriptional repression by miR-1/133, while at the same time, SRF regulates miR-1/133 transcription.^{4,5} Also, the hearts of miR-133a-1/miR-133a-2 double knockout mice are characterized by a number of upregulated genes encoding SM-restricted proteins.¹⁹ On this premise, we first evaluated the direct effects of miR-133 gain (adeno-miR-133 transfection) and loss of function (anti-miR-133) on mRNA and protein levels of 5 SM genes: calponin (CNN1), transgelin-1 (TAGLN1), and -2 (TAGLN2), α -SM actin (also called ACTA2) and SM myosin heavy chain (MYH11 or SM-myosin heavy chain). Accordingly, miR-133 effects on SRF and myocardin expression levels were also evaluated.

miR-133 overexpression decreased the transcript levels of *Cnn1*, *Tagln2*, and *Acta2*, but it actually increased the transcripts of *Myh11* (Figure 4A). Also, adeno-miR-133 had no effect on *Tagln1* mRNA (Figure 4A). It is worth noting here that TAGLN2 is not an SMC-restricted gene, as it is more broadly expressed than TAGLN1, whereas MYH11 is the most specific gene to identify SMCs.¹ These mixed effects at the mRNA level of these SM genes by miR-133 were accompanied by a decrease or increase of the correspondent protein levels (Figure 4B). Accordingly, anti-miR-133 increased mRNA and protein levels of CNN1, TAGLN2 and ACTA2, and it decreased mRNA and protein levels of MYH11 (Figure 4A and 4B).

Furthermore, miR-133 overexpression reduced SRF mRNA and protein levels, whereas the opposite effects were

Figure 4. miR-133 regulation of smooth muscle genes in vitro. **A** and **B**, Effects of Ad-miR-133 and anti-miR-133 on mRNA (**A**) and protein (**B**) levels of calponin (CNN1), transgelin (TAGLN1), transgelin-2 (TAGLN2), α -smooth muscle actin (ACTA2), and smooth muscle myosin heavy chain (MYH11). * $P < 0.05$ vs CTRL; # $P < 0.05$ vs Ad-miR-133. On the right of **B**, representative Western blot of the 5 smooth muscle protein levels in adeno-empty, adeno-miR-133, scrambled anti-miR (Scramb- or Sc-anti-miR), or anti-miR-133-transfected VSMCs. **C**, Effects of Ad-miR-133 and anti-miR-133 on SRF mRNA levels. * $P < 0.05$ vs control (CTRL), Ad-empty, Scramb-anti-miR, and anti-miR-133; # $P < 0.05$ vs CTRL, Ad-empty, Scramb-anti-miR, and adeno-miR-133. **D**, Optical density (OD) of SRF protein levels measured by Western blots as representatively shown on the right. *, # $P < 0.05$ as in **C**. **E**, Effects of Ad-miR-133 and anti-miR-133 on myocardin mRNA levels; $P < \text{not significant}$. **F**, miR-133 levels on PDGF treatment in VSMCs. * $P < 0.05$ vs 0 and 3 hours. **G**, Ad-miR-133 reduced PDGF-induced VSMC proliferation in vitro. * $P < 0.05$ vs BASE; † $P < 0.05$ vs CTRL and Ad-GFP 24 hours. **H**, Ad-miR-133 prevented PDGF-induced smooth muscle gene downregulation in vitro. * $P < 0.05$ vs no PDGF treatment (none, open bars); # $P < 0.05$ vs relative Ad-empty. **I**, Pre-miR-133 effects on Sp-1, Klf4, and myocardin mRNA levels in PDGF-BB-stimulated proliferating VSMCs; * $P < 0.05$ vs no PDGF treatment; # $P < 0.05$ vs relative pre-miR-scrambled. **J**, Sp-1^{mut} and pre-miR-133 overexpression effects on the modulation of Klf-4 and Myocardin levels in proliferating PDGF-BB-stimulated VSMCs in vitro. * $P < 0.05$ vs GFP, pre-miR-scrambled, pre-miR-133, pre-miR-133+GFP, pre-miR-133+Sp-1^{mut}; # $P < 0.05$ vs GFP, Sp-1^{mut}, pre-miR-scrambled, and pre-miR-133+Sp-1^{mut}. **K**, Sp-1^{mut} and pre-miR-133 overexpression effects on the modulation of MYH11 and ACTA2 levels in proliferating VSMCs in vitro. *, # $P < 0.05$ as in **J**.

fostered by the anti-miR-133 (Figure 4C and 4D). Finally, miR-133 does not directly regulate myocardin expression in rat VSMCs in vitro (Figure 4E).

An established model for VSMC phenotypic modulation in vitro involves treatment of VSMCs with PDGF-BB to induce SM gene downregulation and cell proliferation.²⁵ PDGF-BB is known to increase Sp-1 expression and activity, promoting its phosphorylation and nuclear localization.^{22,25} PDGF-BB-activated Sp-1 in turn increases the activity of KLF4 to repress myocardin, toggling SRF from the differentiation to the proliferative program of VSMCs.²² As the differential effects of miR-133 on its own on SM genes and their transcriptional activators and coactivators may also be dependent on the culture in vitro conditions, we tested their interplay in adult rat aortic VSMCs treated with PDGF-BB, which is a proper stimulus to evaluate VSMC phenotypic switch in vitro.

PDGF-BB downregulated miR-133 expression (Figure 4F) and reduced the expression of *Tagln1*, *Acta2*, and *Mylh11*, inducing VSMC proliferation (Figure 4G and 4H). Importantly, adeno-miR-133 prevented PDGF-BB-induced *Tagln1*, *Acta2*, and *Mylh11* downregulation, reducing PDGF-BB-dependent VSMC proliferation (Figure 4G and 4H). Also remarkably, miR-133 overexpression prevented PDGF-BB-induced *Sp-1* and *Klf4* upregulation and *myocardin* downregulation (Figure 4I). When Sp-1^{mut} was overexpressed in VSMCs, miR-133 was unable to prevent PDGF-BB-dependent *Klf-4* upregulation, as well as *myocardin*, *Mylh11*, and *Acta2* downregulation, in proliferating VSMCs in vitro (Figure 4J and 4K).

These data point to miR-133 preventing VSMC phenotypic switch in vitro by specifically repressing Sp-1 expression.

Adeno-miR-133 Transfection in the Rat Carotid Artery Reduces VSMC Phenotypic Switch and Proliferation After Balloon Injury In Vivo

After balloon injury in rats, VSMC activation in the vascular media layer reaches its peak at 2 days.¹⁵⁻¹⁶ At this time point, miR-133 levels were barely detectable in VSMCs of the media layer of injured arteries compared with the uninjured counterparts when evaluated by both quantitative reverse transcription-polymerase chain reaction and FISH (Figure 5A and 5B). miR-133 began to increase in the media layer at 7 days after injury, when it was still absent in neointimal VSMCs (Figure 5A and 5B). Finally, at 14 days, miR-133 was expressed in both medial and neointimal VSMCs (Figure 5A and 5B). On the other hand, miR-1 levels remained unchanged in response to injury (Figure 5A).

Adeno-miR-133 or adeno-miR-1 were intraartery infused, as previously described.^{8,11} Carotid arteries of control rats were transfected with either an adeno-GFP, an adeno-empty, or just saline (labeled as CTRL unless otherwise specifically stated). Adeno-miR-133 transfection increased vascular miR-133 levels 48 hours following balloon injury compared with CTRL. Indeed, adeno-miR-133 normalized miR-133 expression in injured arteries to levels, similar to normal uninjured vessels (Figure 5C). Adeno-miR-1 successfully increased miR-1 vascular expression in injured vessels (Figure 5C).

In the carotid arteries treated with transfection of adeno-miR-133, a significantly lower ratio of Ki-67-positive nuclei to total cells (proliferation index = $3 \pm 2\%$) was observed compared with CTRL carotid vessels (proliferation index = $16 \pm 3.5\%$; $P < 0.05$), 2 days after balloon injury (Figure 5D and 5E). No effects on VSMC proliferation were observed by the transfection of adeno-miR-1 (Figure 5D). Moreover, Sp-1 and moesin were upregulated in carotid arteries following vascular injury (Figure 5F and 5G) compared with uninjured vessels in CTRL rats (Figure 5F and 5G). On the other hand, Sp-1 and moesin injury-induced vascular upregulation was inhibited by adeno-miR-133 treatment in agreement with the destabilizing influence of miRNAs on their specific targets (Figure 5F and 5G).

Thus, miR-133 inversely correlates with VSMC phenotypic switch and proliferation in injured vessels in vivo, and its forced expression reduces VSMC activation after vascular injury, where it negatively regulates the expression of its specific targets, Sp-1 and moesin.

miR-133 Plays a Pivotal Role in Regulating Neointimal Hyperplasia After Balloon Injury In Vivo

In CTRL rats ($n=8$), balloon injury of the carotid artery promoted after 14 days the generation of a thick neointima, which significantly reduced the lumen of the vessel (Figure 6A to 6C). This response was nearly abolished by adeno-miR-133 ($n=7$). Indeed, miR-133 overexpression significantly reduced neointimal hyperplasia (neointimal area = 0.073 ± 0.019 mm², neointima/media ratio = 0.498 ± 0.137) 14 days after experimental balloon angioplasty, compared with CTRL groups (neointimal area = 0.178 ± 0.023 mm², neointima/media ratio = 1.250 ± 0.129) (Figure 6A and 6B). Adeno-miR-1 ($n=7$) had no effect on neointimal formation (neointimal area = 0.180 ± 0.035 mm², neointima/media ratio = 1.190 ± 0.168) (Figure 6A and 6B). In particular, the neointimal tissue of the injured carotid arteries was reduced by $\approx 60\%$ in the rats transfected with adeno-miR-133, compared with CTRL (Figure 6C). The medial layer (0.143 ± 0.014 mm² in CTRL) was not affected by adeno-miR-133 (0.149 ± 0.013 mm², $P =$ not significant), suggesting a normal arterial contractile state. Adeno-GFP ($n=6$) did not affect vascular remodeling per se at 14 days after balloon injury (neointimal area = 0.179 ± 0.018 mm², neointima/media ratio = 1.187 ± 0.132) (Figure 6A to 6C).

To substantiate the inhibitory role played by miR-133 on VSMC proliferation in vivo, we evaluated the effects of antagonizing endogenous miR-133 through the in vivo injection of a PBS-formulated locked-nucleic-acid-modified oligonucleotide to specifically suppress miR-133 (anti-miR-133).²⁶ On the basis of the time course of miR-133 vascular expression after balloon injury (Figure 5A), additional rats were implanted at 7 days after balloon injury with an osmotic pump (under the skin of the rat neck) to systemically release anti-miR-133 (30 mg/kg) from 7 to 14 days. To obtain an in situ time course of vascular cell proliferation within the vessel wall after injury, BrdU was administered intraperitoneally (30 mg/kg) 3 times every 8 hours before each rat euthanasia to label proliferating cells. BrdU-positive VSMCs

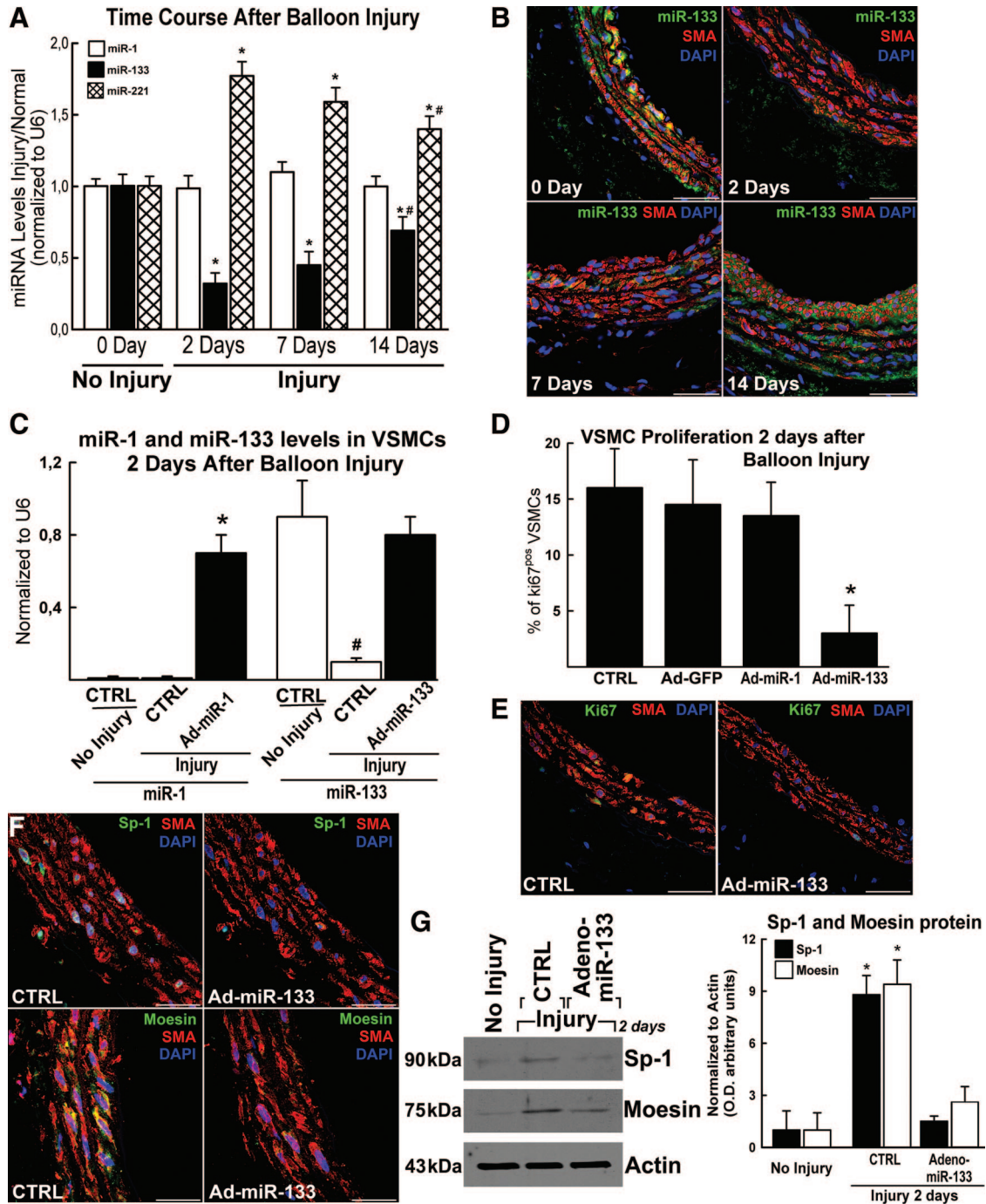


Figure 5. miR-133 regulation of VSMC proliferation in vivo after balloon injury. **A**, miR-133 and miR-1 expression in the vascular wall of uninjured control artery (no injury) at baseline (0 days) at 2 through 14 days after vascular injury. As already reported,¹⁰ miR-221 is significantly upregulated after injury. * $P < 0.05$ vs no injury (0 day); # $P < 0.05$ vs 2 days. **B**, In situ detection of miR-133 expression in rat carotid arteries at 0, 2, 7, and 14 days after balloon injury. 4',6-Diamidino-2-phenylindole (DAPI) (blue) indicates cell nuclei. Scale bars=50 μ m. **C**, Endogenous miR-1 and miR-133 increase by adeno-miR-1 and adeno-miR-133 in vivo transfection. * $P < 0.05$ vs CTRL; # $P < 0.05$ vs no injury CTRL and Ad-miR-133. **D**, Ad-miR-133 significantly reduced VSMC proliferation in vivo. * $P < 0.05$ vs CTRL, Ad-GFP, and Ad-miR-1. **E**, Net reduction of Ki67 positive (green) VSMCs (smooth muscle actin [SMA], red) in Ad-miR-133-treated compared with control (CTRL) rats 2 days after balloon injury. Scale bars=50 μ m. **F**, Moesin and Sp-1 expression (green) in VSMCs (red) was specifically reduced by Ad-miR-133 in vivo 2 days after balloon injury compared with CTRL. Scale bars=50 μ m. **G**, Sp-1 and moesin protein levels were induced at 2 days after balloon damage (injury CTRL) compared with uninjured control (no injury), whereas Ad-miR-133 significantly reduced their induction on injury. * $P < 0.05$ vs no injury and Ad-miR-133.

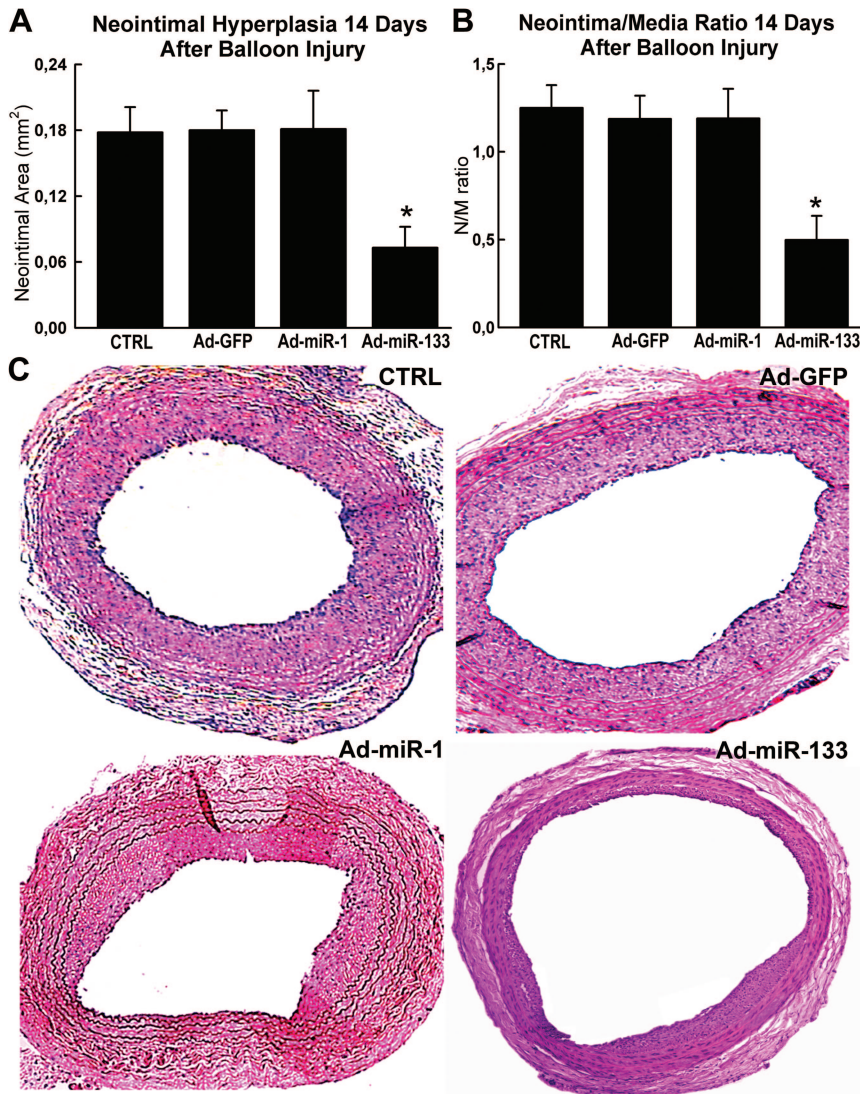


Figure 6. miR-133 overexpression in the rat carotid artery reduces neointimal hyperplasia after balloon injury. **A** and **B**, Neointimal area and neointimal/media (N/M) ratio 14 days after balloon injury. * $P < 0.05$ vs all. **C**, Hematoxylin/eosin staining of carotid cross-sections 14 after balloon injury from the different group of animals included in the adenomiR-133 in vivo study.

reached their peak at 2 days and decreased from 7 to 14 days in the media layer, whereas they peaked at 7 days and decreased thereafter in the neointima layer of CTRL saline-treated animals ($n=4$ for each time point) (Figure 7A and 7B). Anti-miR-133 systemic administration reduced vascular levels of miR-133 at 14 days after injury compared with CTRL (Figure 7C). Importantly, anti-miR-133 treatment ($n=5$) maintained BrdU-positive proliferating VSMCs, which were significantly increased in both media and neointimal layers compared with CTRL at 14 days (Figure 7B). The prolongation of VSMC proliferation by anti-miR-133 resulted in an increased neointimal formation at 14 days after injury (neointimal area = 0.255 ± 0.036 mm², neointima/media ratio = 1.743 ± 0.152) compared with untreated CTRL rats ($n=7$, neointimal area = 0.177 ± 0.021 mm², neointima/media ratio = 1.198 ± 0.132), reducing vessel lumen (Figure 7D to 7F). PBS (saline) lone infusion through the osmotic pump in additional control animals (PBS, $n=6$) did not affect neointimal formation (neointimal area = 0.169 ± 0.029 mm², neointima/media ratio = 1.14 ± 0.143) (Figure 7D to 7F).

Discussion

This study is the first to document the presence of miR-133 in VSMCs and to reveal essential roles of this miRNA in the control of VSMC phenotypic switch in vitro and in vivo. Indeed, (1) miR-133 is robustly expressed in VSMCs to levels similar to other previously characterized vascular miRNAs, whereas the expression of its cognate bicistronic gene, miR-1, is negligible; (2) miR-133 but not miR-1 regulates VSMC growth state by inhibiting VSMC proliferation and migration in vitro; (3) miR-133 specifically targets for repression the transcription factor Sp-1, which mediates miR-133 inhibition of SM gene downregulation and VSMC proliferation in vitro; and (4) miR-133 is downregulated in proliferating VSMCs of carotid arteries in response to balloon injury in rats and adenoviral overexpression of miR-133 in the vascular wall reduces, whereas anti-miR-133 systemic treatment exacerbates VSMC hyperplasia after experimental balloon injury, pointing to a crucial role of miR-133 in regulating pathological vascular remodeling in vivo.

miR-143 and -145 are key players in SM differentiation program through the enhancement of myocardin expression/

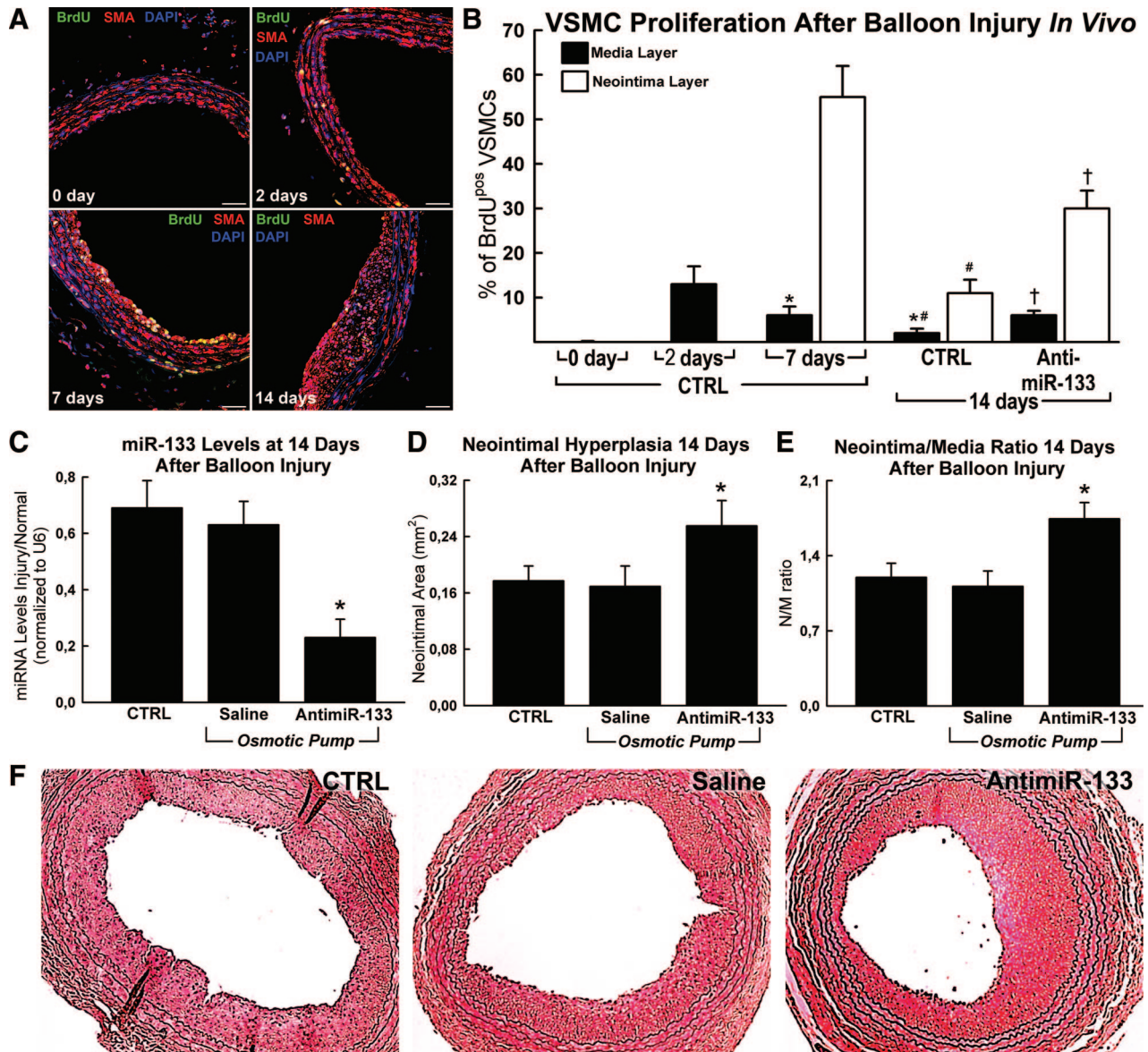


Figure 7. Anti-miR-133 increases VSMC proliferation and neointimal formation after balloon injury. **A**, BrdU-positive (green) VSMCs (smooth muscle actin [SMA], red) in the media and neointima layer before (0 day) and at 2 through 14 days after balloon injury. 4',6-diamidino-2-phenylindole (DAPI), nuclei in blue. **B**, VSMC proliferation (measured as percentage of BrdU^{pos} over total VSMCs) in the media (solid bars) and the neointima (open bars) layers in CTRL (at 2 through 14 days) and anti-miR-133-treated rats. * $P < 0.05$ vs 2 days; # $P < 0.05$ vs 7 days; † $P < 0.05$ vs 14 days. **C**, Anti-miR-133 systemic administration reduced miR-133 vascular levels at 14 days after balloon injury. * $P < 0.05$ vs untreated control (control, no pump [CTRL]) and saline-treated rats. **D** and **E**, Neointimal area and neointimal/media (N/M) ratio. * $P < 0.05$ vs all. **F**, Representative hematoxylin/eosin stainings of carotid cross-sections 14 after balloon injury from the different group of animals included in the anti-miR-133 in vivo study.

activity by silencing the transcription factors Elk4 and Klf4.⁷ miR-145 inhibits SM proliferation and neointima formation after vascular injury, directly repressing KLF5, which in turn regulates myocardin.⁸ Furthermore, miR-145 plays a critical role in keeping the contractile functions of VSMCs and vessels through its regulation of the angiotensin-converting enzyme gene.¹⁰ Finally, miR-143/145 knockout mice present severe structural modifications of the aorta, and accordingly, human aortic aneurysms are characterized by a significant reduced expression of miR-143/145, pointing to a specific role of this miRNA in vascular diseases.⁹ In the present study, we have shown that miR-133 prevents smooth muscle phenotypic switch through direct repression of the transcription

factor Sp-1, which is a known regulator of the Klf4/myocardin axis. Therefore, it is highly tempting to speculate that a miRNA network involving miR-143/145 and miR-133 might exist to cooperatively regulate VSMC phenotypic switch in vitro and in vivo. miR-133 promotes myoblast growth, which suppresses differentiation,^{4,5} whereas it suppresses proliferation of cardiac myocytes by repressing cyclin D2 expression.¹⁹ Here we show that miR-133 robustly decreases rat VSMC proliferation in vitro and following balloon injury in vivo. Also, we have data to show that miR-133 is able to replicate its effects in rat VSMCs also in human coronary-derived SMCs (Online Figure VI). Therefore, miR-133 appears to have both positive and

negative effects on proliferation, depending on the muscle cell type.

Bicistronic genes, such as miR-143/145 and miR-221/222, show similar changes in expression in the vessel wall. However, this was not the case for miR-1/miR-133, as VSMC miR-1 expression is very weak compared with miR-133. Accordingly, previous data show that miR-133 is downregulated in the carotid artery tissue subjected to damage, whereas miR-1 was not reported by the miRNA array as being negligible in the arterial wall.⁶ However, no further analysis was performed to identify either the cellular specificity of miR-133 expression within the vessel wall or its function. Importantly, a differential expression for polycistronic mature miRNAs has already been reported for miR-21 and miR-17 to -92.²⁷ Another intriguing possibility is that miR-1 is actively extruded from VSMCs in a way similar to what happens for other miRNAs shuttled out of the cells through exosomes.²⁸

Two recent articles^{12,13} support a molecular network whereby miR-1 is induced by myocardin overexpression to act as a self-limiting mechanism of myocardin in the regulation of SMC contraction. Indeed, miR-1 expression reduced the proliferation of myocardin-overexpressing human SMCs. However, miR-1 alone only slightly reduces human SMC growth in vitro, whereas anti-miR-1 in absence of myocardin overexpression does not have any effect on hSMC proliferation. Finally, miR-1 expression appears to be downregulated in the vascular wall of ligated common carotid vessels. The data above are only in part at odds with the findings of our present study. First, the data from Zheng group^{12,13} are consistent with our findings in showing minimal if not negligible levels of miR-1 in normal quiescent human SMCs. Second, miR-1 effects on human SMC proliferation are mainly secondary to myocardin overexpression.^{12,13} Third, in the latter 2 studies, 2 different human SMC lines were obtained through in vitro selection, which may have a role in the reported findings. Finally, it should be noted that we injured carotid vessel by balloon endothelial denudation and media injury which is different from the mouse carotid ligation model used by Chen et al.¹³ Accordingly, the reduced expression of miR-1 in the vascular wall after carotid ligation cannot be accounted for by specific variation within SMCs, as it may depend on other cell types within the vessel tissue.

miRNAs mediate important gene-regulatory events by pairing to the mRNAs of protein-coding genes to direct their repression. Here, we showed that miR-133a suppresses the expression of the transcription factor Sp-1 and of the actin-binding protein moesin. In particular, for its central role in modulating VSMC phenotypic switch in vitro and in vivo, we have therefore focused our attention on Sp-1. Sp-1 is indeed a transcription factor activated by phenotypic switch promoting stimuli^{1,3} on which it specifically binds the G/C suppressor cis-element located in MHY11 and TAGLN-1.^{1,20–22} Activated Sp-1 in turn increases the activity of Klf4, which represses myocardin and therefore downregulates most of the SM genes.^{22,25} Furthermore, Sp-1 binding to the G/C repressor element drives SM-gene downregulation after vascular injury in vivo.²⁵ Here, we show that Sp-1 repression by miR-133 is the dominant factor underlying miR-133 effects on SM gene regulation and VSMC proliferation in vitro

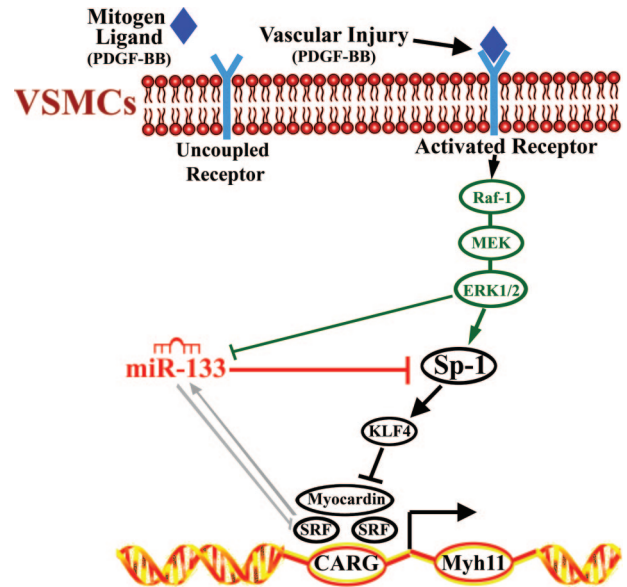


Figure 8. Proposed miR-133-dependent regulation of VSMC phenotypic switch. Vascular injury (through the action of environmental local cues such as mitogen ligands, ie, PDGF-BB) activates a molecular receptor-kinase network, including the sequential activation of the MAPK pathway, which drives VSMC phenotypic switch. Phosphorylation and activation of the transcription factor Sp-1, in turn, activates Klf-4-dependent myocardin downregulation/displacement from the SRF complex determining the downregulation of smooth muscle genes, like smooth muscle myosin heavy chain (MHY11). miR-133 is inhibited by MAPK/ERK1/2 in PDGF-BB-stimulated VSMCs. However, when miR-133 is upregulated (or physiologically active in quiescent cells), it targets Sp-1 for repression, blocking Klf-4 expression and following myocardin repression. Thus, targeting Sp-1, miR-133 inhibits VSMC phenotypic switch, preventing MYH11 (as well as other smooth muscle genes) downregulation and VSMC proliferation. MEK indicates MAPK kinase.

(Figure 8). Indeed, miR-133 gain- and loss-of-function experiments in unstimulated VSMCs show that this miR robustly increases MHY11 (which is the most restricted SM gene) while mildly reducing ACTA2. Accordingly, miR-133 prevents PDGF-BB-induced downregulation of MHY11, ACTA2, and TAGLN1 and VSMC proliferation in vitro. Importantly, when a mutated form of Sp-1, which cannot be targeted for repression by miR-133, is overexpressed in VSMCs, miR-133 loses its function of maintaining the molecular differentiation program and the cellular quiescent state.

A long-standing paradox in vascular biology is the double role of SRF both on VSMC proliferation and differentiation.^{1,3,29} Indeed, SRF regulates growth-responsive genes, such as c-fos, but it also regulates virtually every SMC-specific gene.^{1,3,29} Myocardin is the main SRF coactivator to direct SRF to function as a positive regulator of differentiation, competing with other SRF cofactors, such as Elk-1, Klf4, and others that promote SRF to function as a regulator of proliferation.²⁴ miR-133 is a direct transcriptional target of SRF.^{4,5} However, the genetic interaction between miR-133 and SRF constitutes a negative feedback loop in which the upregulation of miR-133 by SRF results in increased repres-

sion of SRF.^{4,5} Here, we show that miR-133 reduces SRF levels in VSMCs in vitro (Figure 8). However, SRF levels are not crucial for SM gene regulation and VSMC proliferation.^{1,3,29} More importantly, miR-133 targeting Sp-1, which is needed for Klf4 activation to downregulate myocardin,²² prevents myocardin repression and VSMC proliferation on PDGF-BB stimulation in vitro.

Finally, the mechanisms regulating miR-133 expression in muscle cells are only partially known. Indeed, in cardiac and skeletal muscle cells, miR-133 is regulated by several transcription factors or kinases, such as MEF2,³⁰ myogenic regulatory factors, MAPK/ERK1/2,¹⁷ and nuclear factor of activated T cells.³¹ All of these factors are intertwined with SRF,^{1,3} which, as mentioned above, regulates miR-133 expression. Accordingly, the present results suggest that MAPK/ERK1/2 is a critical upstream signaling pathway of miR-133 expression in VSMCs that is responsible for its downregulation when VSMCs are primed for the phenotypic switch in vitro.

Acknowledgments

The authors sincerely thank Bernardo Nadal-Ginard for the helpful comments and suggestions.

Sources of Funding

This work was supported in part by grants from the Italian Ministry of University and Research (PRIN 2007WS3JL3), FIRB-Futuro in Ricerca (RBF081CCS), the Italian Ministry of Health (Ricerca Finalizzata 2007, APICE Project), and Associazione Italiana per la Ricerca sul Cancro (AIRC-MFAG-2008).

Disclosures

None.

References

- Owens GK, Kumar MS, Wamhoff BR. Molecular regulation of vascular smooth muscle cell differentiation in development and disease. *Physiol Rev*. 2004;84:767–801.
- Indolfi C, Mongiardo A, Curcio A, Torella D. Molecular mechanisms of in-stent restenosis and approach to therapy with eluting stents. *Trends Cardiovasc Med*. 2003;13:142–148.
- Miano JM. Serum response factor: toggling between disparate programs of gene expression. *J Mol Cell Cardiol*. 2003;35:577–593.
- Latronico MV, Catalucci D, Condorelli G. Emerging role of microRNAs in cardiovascular biology. *Circ Res*. 2007;101:1225–1236.
- Liu N, Olson EN. MicroRNA regulatory networks in cardiovascular development. *Dev Cell*. 2010;18:510–525.
- Ji R, Cheng Y, Yue J, Yang J, Liu X, Chen H, Dean DB, Zhang C. MicroRNA expression signature and antisense-mediated depletion reveal an essential role of microRNA in vascular neointimal lesion formation. *Circ Res*. 2007;100:1579–1588.
- Cordes KR, Sheehy NT, White MP, Berry EC, Morton SU, Muth AN, Lee TH, Miano JM, Ivey KN, Srivastava D. miR-145 and miR-143 regulate smooth muscle cell fate and plasticity. *Nature*. 2009;460:705–710.
- Cheng Y, Liu X, Yang J, Lin Y, Xu DZ, Lu Q, Deitch EA, Huo Y, Delphin ES, Zhang C. MicroRNA-145, a novel smooth muscle cell phenotypic marker and modulator, controls vascular neointimal lesion formation. *Circ Res*. 2009;105:158–166.
- Elia L, Quintavalle M, Zhang J, Contu R, Cossu L, Latronico MV, Peterson KL, Indolfi C, Catalucci D, Chen J, Courtneidge SA, Condorelli G. The knockout of miR-143 and -145 alters smooth muscle cell maintenance and vascular homeostasis in mice: correlates with human disease. *Cell Death Differ*. 2009;16:1590–1598.
- Boettger T, Beetz N, Kostin S, Schneider J, Krüger M, Hein L, Braun T. Acquisition of the contractile phenotype by murine arterial smooth muscle cells depends on the Mir143/145 gene cluster. *J Clin Invest*. 2009;119:2634–2647.
- Liu X, Cheng Y, Zhang S, Lin Y, Yang J, Zhang C. A necessary role of miR-222 and miR-221 in vascular smooth muscle cell proliferation and neointimal hyperplasia. *Circ Res*. 2009;104:476–487.
- Jiang Y, Yin H, Zheng XL. MicroRNA-1 inhibits myocardin-induced contractility of human vascular smooth muscle cells. *J Cell Physiol*. 2010;225:506–511.
- Chen J, Yin H, Jiang Y, Radhakrishnan SK, Huang ZP, Li J, Shi Z, Kilsdonk EP, Gui Y, Wang DZ, Zheng XL. Induction of microRNA-1 by myocardin in smooth muscle cells inhibits cell proliferation. *Arterioscler Thromb Vasc Biol*. 2011;31:368–375.
- Carè A, Catalucci D, Felicetti F, Bonci D, Addario A, Gallo P, Bang ML, Segnalini P, Gu Y, Dalton ND, Elia L, Latronico MV, Høydal M, Autore C, Russo MA, Dorn GW II, Ellingsen O, Ruiz-Lozano P, Peterson KL, Croce CM, Peschle C, Condorelli G. MicroRNA-133 controls cardiac hypertrophy. *Nat Med*. 2007;13:613–618.
- Indolfi C, Torella D, Coppola C, Curcio A, Rodriguez F, Bilancio A, Leccia A, Arcucci O, Falco M, Leosco D, Chiariello M. Physical training increases eNOS vascular expression and activity and reduces restenosis after balloon angioplasty or arterial stenting in rats. *Circ Res*. 2002;91:1190–1197.
- Torella D, Gasparri C, Ellison GM, Curcio A, Leone A, Vicinanza C, Galuppo V, Mendicino I, Sacco W, Aquila I, Surace FC, Luposella M, Stillo G, Agosti V, Cosentino C, Avvedimento EV, Indolfi C. Differential regulation of vascular smooth muscle and endothelial cell proliferation in vitro and in vivo by cAMP/PKA-activated p85alpha^{PI3K}. *Am J Physiol Heart Circ Physiol*. 2009;297:H2015–H2025.
- Sweetman D, Goljanek K, Rathjen T, Oustanina S, Braun T, Dalmay T, Münsterberg A. Specific requirements of MRFs for the expression of muscle specific microRNAs, miR-1, miR-206 and miR-133. *Dev Biol*. 2008;321:491–499.
- Zhan Y, Kim S, Izumi Y, Izumiya Y, Nakao T, Miyazaki H, Iwao H. Role of JNK, p38, and ERK in platelet-derived growth factor-induced vascular proliferation, migration, and gene expression. *Arterioscler Thromb Vasc Biol*. 2003;23:795–801.
- Liu N, Bezprozvannaya S, Williams AH, Qi X, Richardson JA, Bassel-Duby R, Olson EN. microRNA-133a regulates cardiomyocyte proliferation and suppresses smooth muscle gene expression in the heart. *Genes Dev*. 2008;22:3242–3254.
- Madsen CS, Hershey JC, Hautmann MB, White SL, Owens GK. Expression of the smooth muscle myosin heavy chain gene is regulated by a negative-acting GC-rich element located between two positive-acting serum response factor-binding elements. *J Biol Chem*. 1997;272:6332–6340.
- Madsen CS, Regan CP, Owens GK. Interaction of CArG elements and a GC-repressor element in transcriptional regulation of the smooth muscle myosin heavy chain gene in vascular smooth muscle. *J Biol Chem*. 1997;272:29842–29851.
- Deaton RA, Gan Q, Owens GK. Sp1-dependent activation of KLF4 is required for PDGF-BB-induced phenotypic modulation of smooth muscle. *Am J Physiol Heart Circ Physiol*. 2009;296:H1027–H1037.
- Blind R, Zeiffer U, Krott N, Filzmaier K, Voss M, Hanrath P, vom Dahl J, Bosserhoff AK. Up-regulation of the cytoskeletal-associated protein Moesin in the neointima of coronary arteries after balloon angioplasty: a new marker of smooth muscle cell migration. *Cardiovasc Res*. 2002;54:630–639.
- Parmacek MS. Myocardin-related transcription factors: critical coactivators regulating cardiovascular development and adaptation. *Circ Res*. 2007;100:633–644.
- Wamhoff BR, Hoofnagle MH, Burns A, Sinha S, McDonald OG, Owens GK. A G/C element mediates repression of the SM22alpha promoter within phenotypically modulated smooth muscle cells in experimental atherosclerosis. *Circ Res*. 2004;95:981–988.
- Elmén J, Lindow M, Schütz S, Lawrence M, Petri A, Obad S, Lindholm M, Hedtjörn M, Hansen HF, Berger U, Gullans S, Kearney P, Sarnow P, Straarup EM, Kauppinen S. LNA-mediated microRNA silencing in non-human primates. *Nature*. 2008;452:896–899.
- Newman MA, Hammond SM. Emerging paradigms of regulated microRNA processing. *Genes Dev*. 2010;24:1086–1092.
- Pegtel DM, Cosmopoulos K, Thorley-Lawson DA, van Eijndhoven MA, Hopmans ES, Lindenberg JL, de Gruijld TD, Würdinger T, Middeldorp

- JM. Functional delivery of viral miRNAs via exosomes. *Proc Natl Acad Sci U S A*. 2010;107:6328–6333.
29. Miano JM. Role of serum response factor in the pathogenesis of disease. *Lab Invest*. 2010;90:1274–1284.
30. Liu N, Williams AH, Kim Y, McAnally J, Bezprozvannaya S, Sutherland LB, Richardson JA, Bassel-Duby R, Olson EN. An intragenic MEF2-dependent enhancer directs muscle-specific expression of microRNAs 1 and 133. *Proc Natl Acad Sci U S A*. 2007;104:20844–20849.
31. Dong DL, Chen C, Huo R, Wang N, Li Z, Tu YJ, Hu JT, Chu X, Huang W, Yang BF. Reciprocal repression between microRNA-133 and calcineurin regulates cardiac hypertrophy: a novel mechanism for progressive cardiac hypertrophy. *Hypertension*. 2010;55:946–952.

Novelty and Significance

What Is Known?

- Adult vascular smooth muscle cells (VSMCs) possess remarkable plasticity and can undergo reversible changes in phenotype and growth properties in response to changes in local environmental cues. This phenotype switching contributes to vascular disease, including atherosclerosis, restenosis, cancer, and hypertension.
- VSMC phenotypic switch is characterized by significant changes in gene expression, matrix and cytokine production, and contractility and growth state.
- MicroRNAs (miRNAs) are short (≈ 22 -nucleotide), noncoding RNA molecules with the general function of translational repression and gene silencing.

What New Information Does This Article Contribute?

- MicroRNA-133 (miR-133, previously reported to be restricted to cardiac and skeletal muscle) is robustly expressed in VSMCs, whereas the expression of its cognate bicistronic gene, miR-1, is negligible.
- miR-133 regulates VSMC phenotypic switch by inhibiting VSMC proliferation and maintaining smooth muscle gene differentiation program.
- Vascular overexpression of miR-133 reduces neointimal hyperplasia after experimental balloon injury.

The understanding of the regulatory mechanisms that underlie VSMC phenotypic switch in response to vascular injury is of paramount importance in designing effective therapies for vascular disease. Several miRNAs regulate key genetic programs in vascular development and disease. The bicistronic miR-1/miR-133 gene plays a fundamental role in skeletal and cardiac muscle biology, but its function in vascular smooth muscle remains unknown. We show here for the first time that miR-133 is expressed in VSMCs and that miR-133 plays an essential role in regulating VSMC phenotypic in vitro and in vivo. miR-133 is robustly expressed in VSMCs to levels similar to those of other previously characterized vascular miRNAs; however, the expression of its cognate bicistronic gene, miR-1, is negligible. We found that miR-133 inhibits VSMC proliferation by repressing the transcription factor Sp-1 and that it prevents smooth muscle gene downregulation on mitogen stimuli. miR-133 is downregulated in proliferating VSMCs of carotid arteries in response to balloon injury in rats, and overexpression of miR-133 in the vascular wall reduces neointimal hyperplasia after experimental balloon injury. These findings point to a crucial role of miR-133 in regulating pathological vascular remodeling and open new avenues for the use of miR-133 in the treatment of vasculoproliferative diseases.

SUPPLEMENTARY INFORMATION

Methods

Adenovirus, cell culture, and reagents

Adenoviruses expressing miR-1 (abbreviated as Adeno-miR-1 or Ad-miR-1) and miR-133 (Adeno-miR-133 or Ad-miR-133) were obtained as previously described (1). Green fluorescent protein (GFP) adenovirus vector (Adeno-GFP) or adeno-empty was used as control reporter gene and control virus, respectively. GFP plasmid construct and the SP-1 cDNA construct mutated in the 3'UTR binding site for miR-133 seed region (Sp-1^{mut}) were obtained from Origene. The synthetic miR-133 mimic (pre-miR-133 precursor molecule) and the scrambled pre-miR were obtained from Ambion. Adult rat aortic vascular smooth muscle cells (2) were grown in DMEM supplemented with 10% fetal bovine serum (FBS, Gibco). Adenoviruses were transfected as previously reported (1). Efficiency of the transfection of the reporter gene adenoconstruct *in vitro* was evaluated by flow-activated cell sorting (FACS) (3). Anti-miRTM to miR-1 and miR-133 (AntimiR-1 and AntimiR-133, respectively) and negative control 1 (a scrambled oligonucleotide, Scrambled-AntimiR) were obtained from Ambion (Austin, Texas). The AntimiR-1, AntimiR-133, Scrambled-AntimiR, pre-miR-133 and Scrambled-pre-miR were introduced into the cells by reverse transfection using the transfection agent siPORTTM NeoFXTM (Ambion). Cell culture media was changed after 8 hours to remove the transfection reagent in an attempt to avoid toxicity which may be caused by NeoFXTM. All the *in vitro* experiments were performed in quadruplicate, and the data shown as Average \pm StDev.

Determination of RNA Levels by Quantitative RT-PCR

miRNAs/ mRNAs were extracted from rat adult aortic VSMCs, aortas, carotid arteries, bronchial tissues hearts, and skeletal muscle isolated from male Wistar Rats. Specifically, for miRNA/ mRNA extraction from isolated cells, mirVanaTM miRNA Isolation Kit (Ambion, Inc) was used while Trizol was employed for miRNA/mRNA extraction from solid tissues. Specific cDNA was obtained using the high-capacity cDNA Reverse transcription kit (Applied Biosystems). TaqMan[®] MicroRNA Assays (Ambion) and TaqMan[®] Gene Expression Assays (Ambion) or SYBR-GREEN (Biorad) were used to quantify miRNAs (miR-1, miR-133a, miR-133b, miR-143, miR-145, miR-221 and miR-222) and mRNA levels, respectively, by quantitative (q)RT-PCR. Finally, specific localization of mature miR-133 within VSMCs was further evaluated by separating cytoplasmic content from nuclei (4)

The specific sequences of the primers used are the following: calponin, (F) TAGAGCTTGCAGATGGGGAGCAA – (R) TGGGAAAGCTCCAGGGATGA; alpha smooth muscle actin, ACTA2, (F) ATCCGATAGAACACGGCATC - (R) AGGCATAGAGGGACAGCACA; smooth muscle heavy chain, SM-MHC (MYH11), (F) CAGTTGGACACTATGTCAGGGAAA - (R) ATGGAGACAAATGCTAATCAGCC; transgelin-1, TAGLN-1, (F) GCATAAGAGGGAGTTCACAGACA - (R) GCCTTCCCTTTCTAACTGATGATC; transgelin-2, TAGLSN-2, (F) GCTGGCATCCGCCGAGTG - (R) GCACCTTACCAGGGTCCAATGT; serum SRF, (F) CCAGCGCTGTCAGCAGTGCCAAC - (R) GCTGCTCCCAGCTTGCTGCCCTATC-3'; GAPDH, (F) ACCACAGTCCATGCCATCAC' - (R) TCCACCACCTGTTGCTGTA.

In vitro Cell Assays

For cell proliferation, transfected VSMCs were serum starved (0% FBS) for 36-48 hours; then, normal serum medium (10% FBS) was added. BrdU (10 μ m/L) was added every eight hours.

At different time points, cells were fixed and stained to detect cell proliferation, according to the manufacturer's instructions (Roche) (3). The percentage of BrdU-positive VSMCs (relative to total cells) was determined by counting ~1000 cells in 10 randomly chosen fields/dish. In parallel experiments, cell counts at time 0 (Baseline, BASE) and at 12, 24, 48 and 96 hours were obtained as previously described (5).

Cell proliferation was measured by two different assays to obtain complimentary data. It is indeed well-documented that using this protocol, the BrdU nucleoside disappear from the media in a manner of minutes and do not produce continuous labeling of the cells but short pulse labeling, that's why is necessary to re-spike the media at intervals shorter than the S phase of the cells under study to have a chance to label most of those that enter the cell cycle (6). Thus, the BrdU assay, as above detailed, responds to the question at a single cell level on how miR-133/miR-1 affect VSMCs primed to re-enter the cell cycle (within the known cell cycle period lasting less than 24-hours for this cell type). On the other hand, cell counts at 48 hours show the net effects of miR-133/miR-1 on VSMC proliferation as a whole cell population.

VSMC migration was assayed by a modification of the Boyden's chamber method as previously described (5). Rat VSMCs were placed in the upper chamber, and DMEM containing 10% serum as general migration factor was placed in the lower chamber. At the end of the assay period, VSMCs that had migrated to the lower side of the filter were counted under a microscope to quantify VSMC migration.

VSMC activation (proliferation and migration) is secondary to a multitude of growth factors and therefore we primarily set the experiments to evaluate any role of miR-133 on VSMCs primed to proliferate/migrate in response to 10% serum. On the other hand, to directly evaluate VSMC phenotypic switch *in vitro*, we used an experimental *in vitro* model of VSMC modulation, which entails cell stimulation by PDGF-BB, which is also a known mitogen for VSMCs directly down-regulates main VSMC genes (7).

Luciferase Reporter and Activity Assay

A fragment of the 3' un-translated region (3'-UTR) of Sp-1 or Moesin containing the putative predicted miR-133 binding site was ligated into the pMiR-Reporter vector (Ambion) 3' of the luciferase gene. As a negative control, three mutations were introduced into the seed region of miR-133 binding site of the Sp-1 or Moesin sequence. Adult rat VSMCs cells were plated at 10×10^4 in 24-well cell culture plates. The pMir-Reporter containing the Sp-1 or Moesin binding site for miR-133 were co-transfected with either pre-miR-133, a scrambled miRNA, AntimiR-133 or Scrambled AntimiR (Ambion) using Lipofectamine 2000. Control cells (CTRL) were treated with lipofectamine 2000 alone. All experiments were also co-transfected with β -galactosidase vector as a control for transfection efficiency and normalization. Luciferase activity was measured by One-Glo luciferase assay (Promega) according to manufactures instructions and as previously described (8).

Western blot Analysis

Proteins were isolated from cultured VSMCs or carotid arteries and protein levels were determined by SDS-PAGE and Western blot analysis as previously described (3,9). The antibodies used were the following: rabbit anti-Moesin (Cell Signaling), mouse anti-SP-1, mouse anti-ACTA2, rabbit anti-TAGLN-1, mouse TAGLN-2, mouse anti-calponin, mouse anti-SRF, goat anti-GAPDH (Santa Cruz Biotech) and mouse anti-MYH11 (BT-562, Biomedical Technologies).

Animal study design and experimental balloon injury

The animals in this study were handled according to the animal welfare regulation of the Magna Graecia University of Catanzaro, and the protocol was approved by the animal use committee of this Institution. Balloon injury of the right carotid artery was performed in male Wistar rats (weighing 330±30g, Harlan Italy) using a Fogarty 2F arterial embolectomy catheter (Baxter Healthcare Corp.) as described (3,9). After the vascular injury, the balloon-dilated common carotid arteries were randomly infused through the external carotid artery with the specific adenoviral constructs (10,11). The rats received the following constructs after balloon injury: adeno-miR-1, adeno-miR-133, adeno-empty vector alone or adeno-GFP. In additional rats, just saline was infused (CTRL). Also, additional carotid arteries isolated at 2 days after balloon injury (n=5 for each group) were dissociated and RNA extracted for real time qRT-PCR analysis of miR-1/-133 vascular expression *in vivo* (3,9).

In the miR-133 loss of function experiments *in vivo*, osmotic mini-pumps (Alzet) were implanted under the skin of the rat neck for a 1-week continuous infusion of PBS-formulated LNA-modified AntimiR-133 (Exiqon), or just phosphate buffered saline (PBS).

Tissue Immunohistochemistry and Morphological Characteristics

After completion of the relative *in vivo* studies, the rat abdominal aorta was cannulated and perfused with 10% buffered formalin (3,8). The isolated carotid arteries were embedded in paraffin and 5µm cross sections were prepared on a microtome (Leica, RM2235).

VSMC proliferation was assessed by staining 2-day balloon injured arteries (n= 5 for each group) for ki67 (3,8). Ki67 was detected using a rabbit polyclonal antibody against Ki67 (1:50 dilution; Vector Labs) overnight at 4°C. A proliferation index (PI) was defined as the number of Ki67 positive cell nuclei in the tunica media divided by the total number of cell nuclei. Proliferating and newly formed VSMCs in the media as well as neointimal layers were detected through double staining for BrdU and α-smooth muscle actin. BrdU was detected using an antibody against BrdU (1:50 dilution; Roche). Vascular smooth muscle cells were detected using an antibody against smooth muscle (SM) α-actin (Sigma). Sp-1 and Moesin were respectively detected with rabbit polyclonal antibodies against Sp-1 (1:50 dilution; Santa Cruz) and Moesin (1:50 dilution; Cell Signaling) overnight at 4°C. For anatomical and morphological measurements, 14 days after balloon-injury, EEL (external elastic membrane), IEL (internal elastic membrane), lumen, media, and neointimal were measured on H&E stained cross sectional carotid artery segments using a computerized image analysis system. The ratios between neointima and media were calculated (3,9). All fluorescence images were analyzed with a Zeiss LSM 710 confocal microscope and Zen 2009 image software.

Detection of miR-133 in Vessel Sections by Fluorescence In Situ Hybridization

Fluorescent in situ hybridizations (FISH) of miR-133 and co-immunofluorescence with the smooth muscle marker alpha smooth muscle actin (αSMA) were performed on 5-µm paraffin-embedded arterial sections. Briefly, paraffin embedded tissue sections were cut using a microtome (Leica, RM2235) and mounted on Polysine microscope slides (Fisher Scientific) and stored at room temperature (RT) until FISH. Paraffin wax was removed in Xylene, sections rehydrated in a series of decreasing ethanol solutions and washed with PBS before fixing in 4% paraformaldehyde. To block endogenous peroxide activity, tissue sections were treated with 0.3% H₂O₂ and washed in PBS before acetylating in acetic anhydride/triethanolamine. Sections were then washed in 2xSSC and PBS before permeabilisation with Proteinase K (5µg/ml) and washes with PBS. Probes (5' & 3'-DIG labelled LNA miRCURY probes; Exiqon) were denatured at 90°C before dilution in

hybridisation buffer (50% formamide, 0.3M NaCl, 20mM Tris-HCL, 5mM EDTA, 10mM NaPO₄, 10% Dextran sulphate, 1xDenhardt's solution, 0.5mg/ml yeast tRNA). Tissue sections were hybridised with miR-133a (200nM) overnight at 21°C below the predicted T_m value of the probe. After post-hybridization washes in 5xSSC at RT; 50% formamide/1xSSC/0.1% Tween 20 at the hybridisation temperature; 0.2xSSC at RT, FISH signals were detected using an Anti-Digoxigenin antibody and the tyramide signal amplification system (PerkinElmer) according to the manufacturer's instructions. To determine co-localization of miR-133a and VSMCs, VSMCs were stained by immunofluorescence of smooth muscle (SM) α -actin (Sigma). Tissue sections were treated with DAPI and mounted in Vectashield (Vector laboratories). All fluorescence images were analyzed with a Zeiss LSM 710 confocal microscope and Zen 2009 image software. To determine the success of the procedure, other tissue sections from the same samples were hybridised with either a 5'-DIG labelled U6 control probe (10nM) or a 5' & 3'-DIG labelled scrambled sequence probe (200nM) to act as positive and negative controls respectively.

Detection of miR-133 in isolated or cultured adult aortic VSMCs by Fluorescence In Situ Hybridization

Freshly isolated aortic VSMCs were isolated and suspended in growth medium. 200 μ l of a 0.5×10^6 cell/ml suspension were directly loaded in each cytofunnel and spun down at 800rpm for 3 minutes onto poly-lysine-coated slides using a Shandon Cytospin 4 Cyto centrifuge (Thermo). Slides were immediately fixed using a spray fixative (Shandon Cell-Fixx, Thermo) and then processed for miR-133 detection by FISH as above described.

Adult aortic VSMCs were cultured on glass chamber slides (BD Falcon), fixed with 4% PFA for 20 min, and then stained as above described.

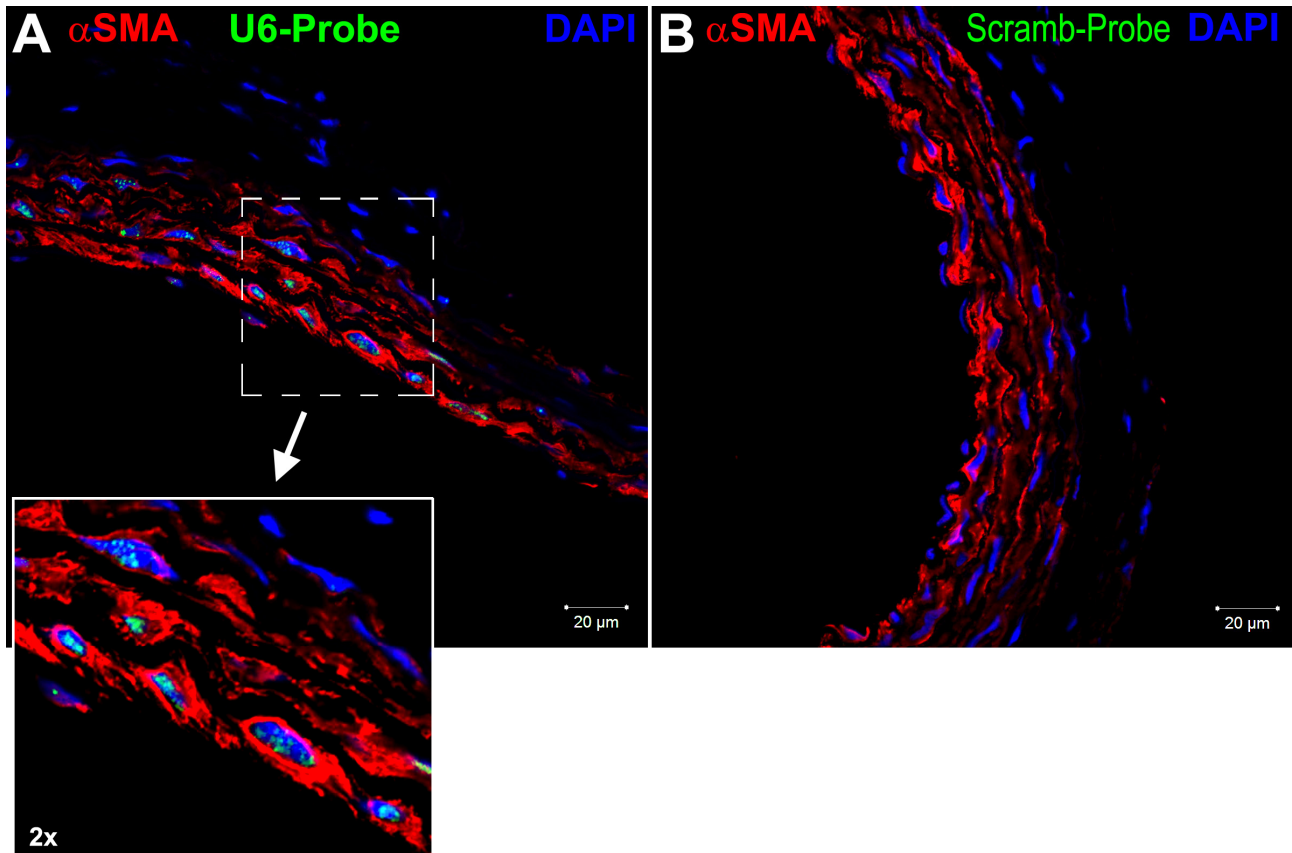
Statistical Analysis

Data was analysed using ANOVA, SPSS version 10.0 (SPSS Inc.). When an significant effect was detected, Bonferroni test was used to compare mean values. A p value of < 0.05 was considered significant.

REFERENCES:

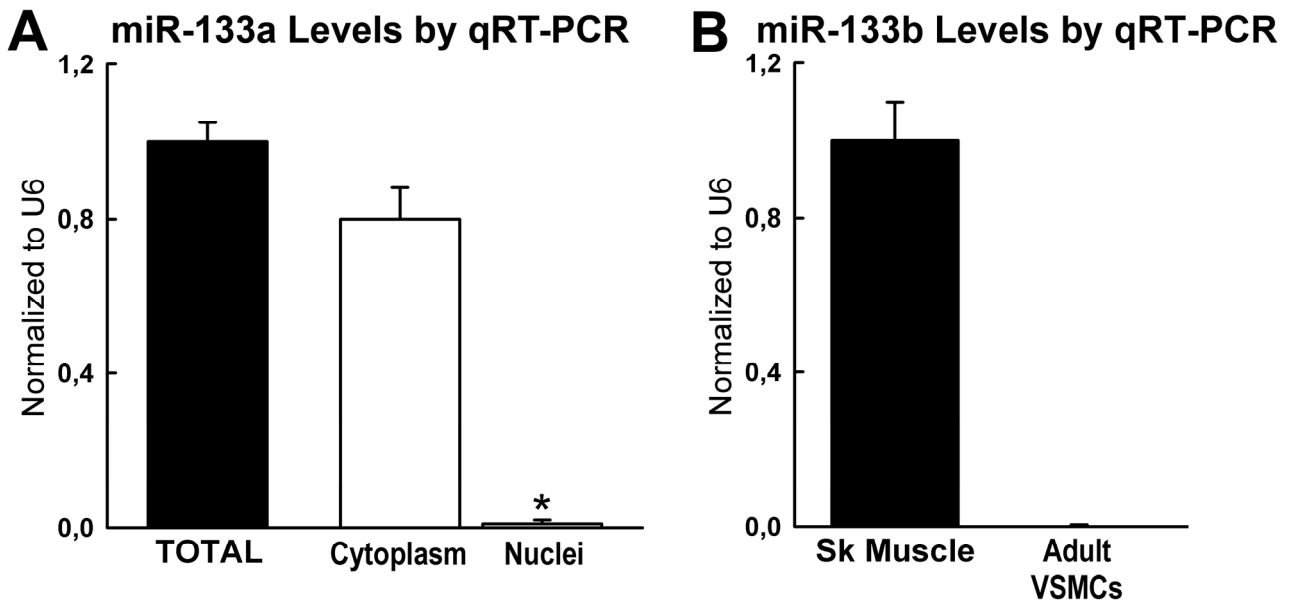
1. Carè A, Catalucci D, Felicetti F, Bonci D, Addario A, Gallo P, Bang ML, Segnalini P, Gu Y, Dalton ND, Elia L, Latronico MV, Høydal M, Autore C, Russo MA, Dorn GW 2nd, Ellingsen O, Ruiz-Lozano P, Peterson KL, Croce CM, Peschle C, Condorelli G. MicroRNA-133 controls cardiac hypertrophy. *Nat Med.* 2007;13:613-618.
2. Curcio A, Torella D, Cuda G, Coppola C, Faniello MC, Achille F, Russo VG, Chiariello M, Indolfi C. Effect of stent coating alone on in vitro vascular smooth muscle cell proliferation and apoptosis. *Am J Physiol Heart Circ Physiol.* 2004;286:H902-908.
3. Torella D, Gasparri C, Ellison GM, Curcio A, Leone A, Vicinanza C, Galuppo V, Mendicino I, Sacco W, Aquila I, Surace FC, Luposella M, Stillo G, Agosti V, Cosentino C, Avvedimento EV, Indolfi C. Differential regulation of vascular smooth muscle and endothelial cell proliferation *in vitro* and *in vivo* by cAMP/PKA-activated p85alpha^{P13K}. *Am J Physiol Heart Circ Physiol.* 2009;297:H2015-2025.
4. Jeffries CD, Fried HM, Perkins DO. Nuclear and cytoplasmic localization of neural stem cell microRNAs. *RNA.* 2011;17:675-686.

5. Indolfi C, Torella D, Cavuto L, Davalli AM, Coppola C, Esposito G, Carriero MV, Rapacciuolo A, Di Lorenzo E, Stabile E, Perrino C, Chieffo A, Pardo F, Chiariello M. Effects of balloon injury on neointimal hyperplasia in streptozotocin-induced diabetes and in hyperinsulinemic nondiabetic pancreatic islet-transplanted rats. *Circulation*. 2001;103:2980-2986.
6. Krauter K, Soeiro R, Nadal Ginard B. Transcriptional regulation of ribosomal RNA accumulation during L6E9 myoblast differentiation. *J. Mol. Biol.* 1979;134:727-740
7. Wamhoff BR, Hoofnagle MH, Burns A, Sinha S, McDonald OG, Owens GK. A G/C element mediates repression of the SM22alpha promoter within phenotypically modulated smooth muscle cells in experimental atherosclerosis. *Circ Res*. 2004;95:981-988.
8. Liu N, Bezprozvannaya S, Williams AH, Qi X, Richardson JA, Bassel-Duby R, Olson EN. microRNA-133a regulates cardiomyocyte proliferation and suppresses smooth muscle gene expression in the heart. *Genes Dev*. 2008;22:3242-3254.
9. Indolfi C, Torella D, Coppola C, Curcio A, Rodriguez F, Bilancio A, Leccia A, Arcucci O, Falco M, Leosco D, Chiariello M. Physical training increases eNOS vascular expression and activity and reduces restenosis after balloon angioplasty or arterial stenting in rats. *Circ Res*. 2002;91:1190-1197.
10. Cheng Y, Liu X, Yang J, Lin Y, Xu DZ, Lu Q, Deitch EA, Huo Y, Delphin ES, Zhang C. MicroRNA-145, a novel smooth muscle cell phenotypic marker and modulator, controls vascular neointimal lesion formation. *Circ Res*. 2009;105:158-166.
11. Liu X, Cheng Y, Zhang S, Lin Y, Yang J, Zhang C. A necessary role of miR-222 and miR-221 in vascular smooth muscle cell proliferation and neointimal hyperplasia. *Circ Res*. 2009; 104: 476–487.

Online Figure I**Online Figure I. FISH positive and negative miR probe controls.**

(A) Nuclear localization of U6 as specifically detected by U6 probe (see insert at higher magnification) in the representative fluorescence in situ hybridization (FISH) analysis of control uninjured rat common carotid artery. U6 probe, green fluorescence; alpha smooth muscle actin (α SMA), red fluorescence; DAPI (blue fluorescence) depicts cell nuclei. (B) As negative control of FISH analysis, a scramble miRNA probe (Scramb-Probe) was employed; the scramble probe could not be detected as demonstrated by the absence of any green fluorescent signal.

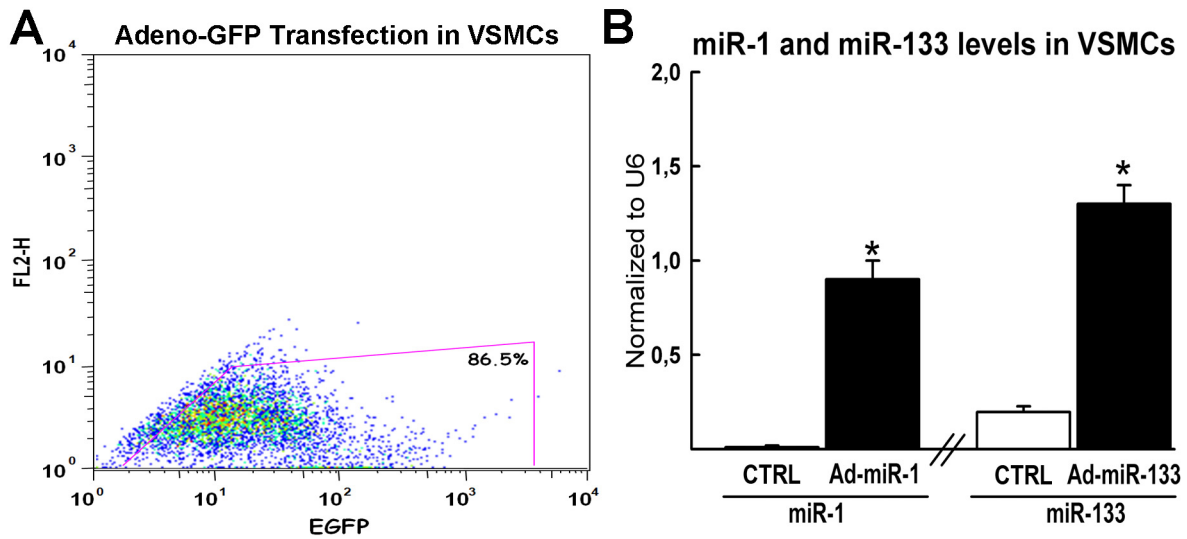
ONLINE FIGURE II



Online Figure II. Intracellular localization of miR133a in VSMCs and miR-133b expression in VSMCs in vitro.

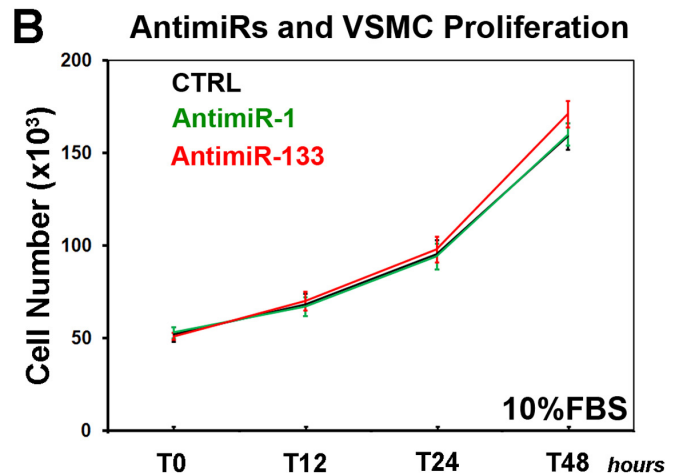
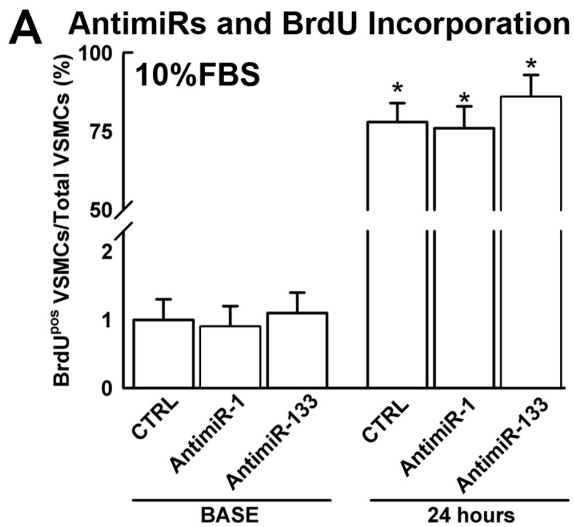
(A) Specific localization of mature miR-133a within VSMCs was evaluated by separating cytoplasmic content from nuclei as previously described (see reference 4). qRT-PCR shows that miR-133 is mainly expressed in the cytoplasm of VSMCs. * $p < 0.05$ vs. all. (B) miR-133b is not expressed in adult rat VSMCs. Skeletal muscle was used as positive control.

ONLINE FIGURE III

**Online Figure III. Adenovirus constructs transfection in VSMCs *in vitro*.**

(A) FACS analysis shows that more than 85% of rat VSMCs were efficiently transfected with the adenoviral vector carrying the control reporter gene for green fluorescent protein (Adeno-GFP). (B) Ad-miR-1 and Ad-miR-133 transfection (50 MOI) significantly increased miR-1 and miR-133 levels in VSMCs *in vitro*. * $p < 0.05$ vs. CTRL.

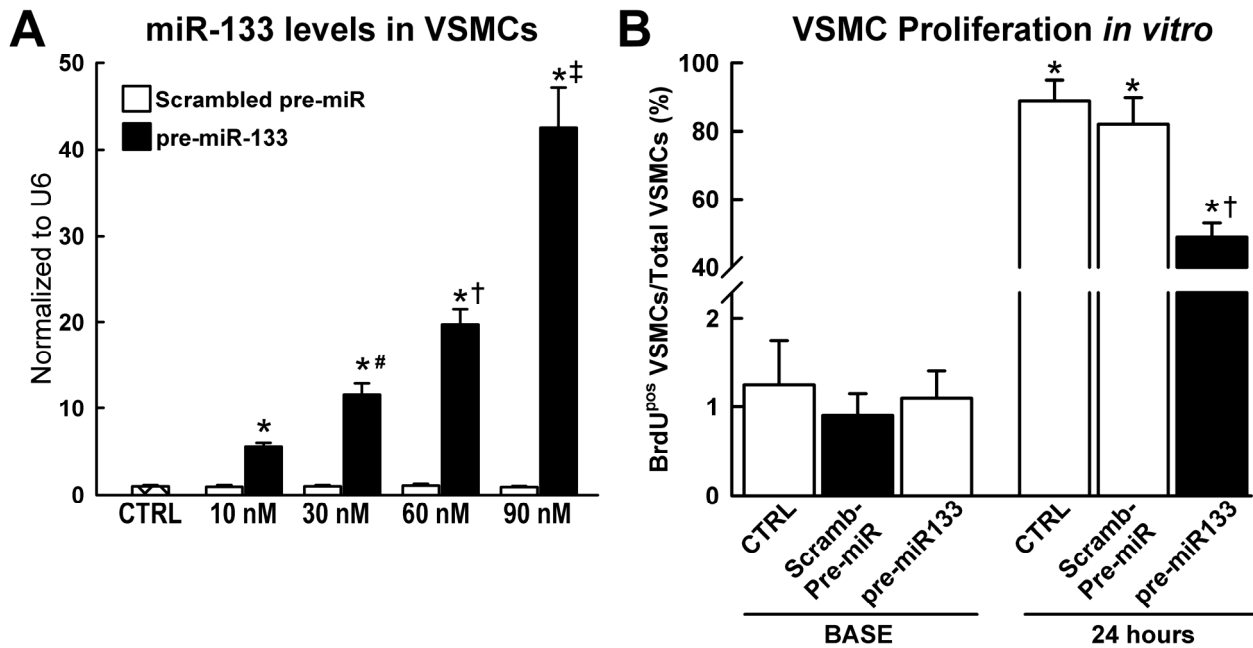
ONLINE FIGURE IV



Online Figure IV. AntimiR-1 and AntimiR-133 effects on VSMC stimulated by 10%FBS *in vitro*. (A-B) AntimiR-1 and AntimiR-133 did not affect 10%FBS-stimulated VSMC proliferation measured through BrdU incorporation (administered 3 times every 8 hours in 24 hours) as well as cell counts. F, * $p < 0.05$ vs. BASE.

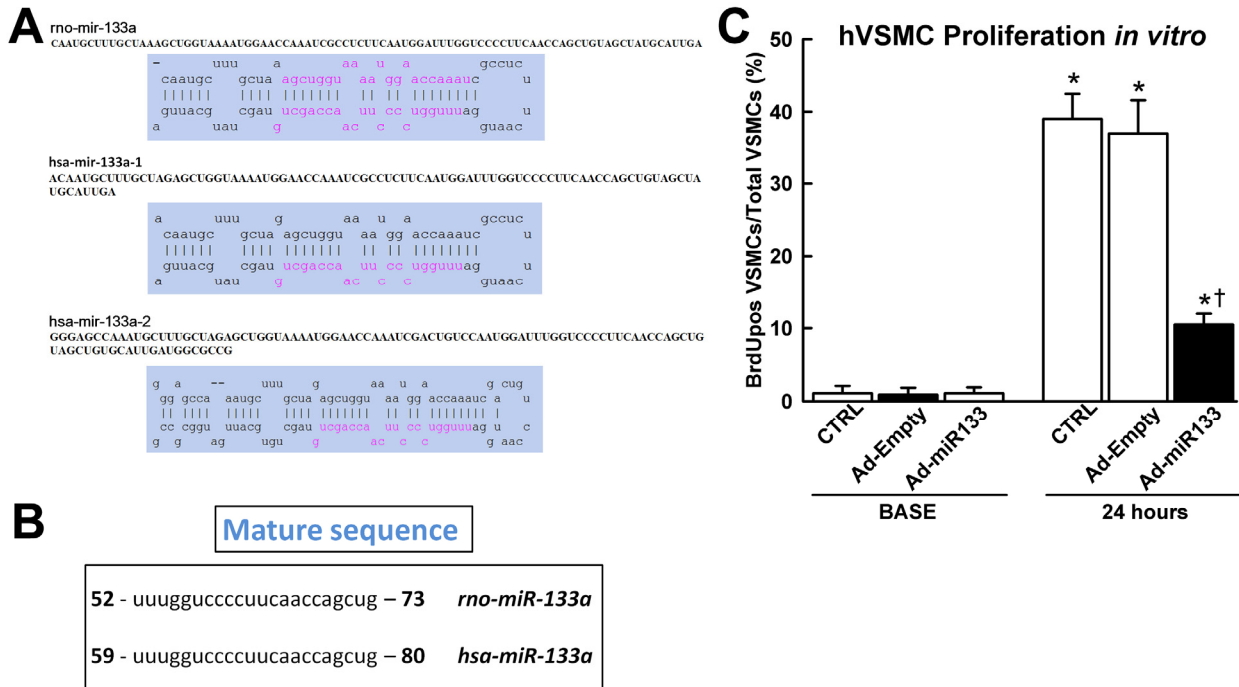
Note. The data in Panel A is presented at 24 hours as percentage of VSMCs labeled by BrdU. The latter represent cells that are within the cell cycle and/or cells that have entered at least once the cell cycle without taking into account the actual cell counts and cell number increase over time.

ONLINE FIGURE V



Online Figure V. Pre-miR-133 overexpression and VSMC proliferation *in vitro*. (A) Pre-miR-133 construct was transfected at different concentrations (10 through 90 nanomolar, nM) in rat adult VSMCs *in vitro* using the transfection agent siPORT™ NeoFX™ (Ambion). As a negative control, a scramble pre-miR sequence was used (Scrambled pre-miR). Pre-miR-133 increases miR-133 levels in a dose dependent manner. * $p < 0.05$ vs. CTRL and Scrambled pre-miR; # $p < 0.05$ vs. 10, 60 and 90 nM; † $p < 0.05$ vs. 10, 30 and 90 nM; ‡ $p < 0.05$ vs. 10, 30 and 60 nM. CTRL refers to untransfected cells, which show the endogenous physiologic levels of miR-133 to compare with the pre-miRs' transfection at the different concentrations. (B) Pre-miR-133 (30nM) reduced 10%FBS-stimulated VSMC proliferation measured through BrdU incorporation (administered 3 times every 8 hours in 24 hours). * $p < 0.05$ vs. BASE; † $p < 0.05$ vs. CTRL and Scramb-Pre-MiR at 24 hours.

ONLINE FIGURE VI



Online Figure VI. Human and Rat miR-133 sequence and miR-133 effects on human vascular smooth muscle cell proliferation. (A) Rattus norvegicus miR-133a stem-loop sequence and homo sapiens (hsa) miR-133a-1 and a-2 stem-loop sequences as available at <http://www.mirbase.org>. (B) The rat and human miR-133a mature sequences are identical. (C) Ad-miR-133 reduced human coronary artery smooth muscle cells (hVSMCs) proliferation *in vitro* as measured BrdU incorporation. B, *p<0.05 vs. BASE; †p<0.05 vs. CTRL and Ad-Empty at 24 hours.